Research on Chemical Intermediates (2023) 49:5163–5203
https://doi.org/10.1007/s11164-023-05119-y

Recent trends of nanocatalyst for organic transformations via sustainable environmental benign route

Reshma P. Patil[1] · **Vilasrao A. Kalantre**[2] · **Krishna N. Alasundkar**[1]

Received: 4 February 2023 / Accepted: 20 August 2023 / Published online: 25 September 2023

Abstract

Nanocatalyst is rapidly developing field and is a key factor of environmentally-safe sustainable technology and organic transformations. An increasing interest is nowadays devoted to the high activity and selectivity of nanocatalyst. Several, attractive candidates as a catalyst are, metal nanocatalysts, metal oxide nanocatalysts, bimetallic nanocatalysts, and supported NPs, deed sustainable idea to conduct divers big chemical transformations in an environmentally friendly aspects. The fringe benefits affiliated with the catalytic applications of nanoparticles in organic synthesis completed beneath very moderate and green conditions. This review goals to present the prevailing crest on the applications of numerous kinds of nanoparticles for organic transformations. At the end, the author's viewpoints are; counting imminent advancement of green, sustainable and efficient chemical processes is one of the biggest crucial challenges in the area of organic synthetic nanotechnology via sustainable environmentally friendly manner.

✉ Krishna N. Alasundkar
korgchem@yahoo.co.in

Reshma P. Patil
reshmapatil20591@gmail.com

Vilasrao A. Kalantre
kalantreva@yahoo.com

[1] Department of Chemistry, Government College of Engineering, Karad, Maharashtra, India

[2] Balasaheb Desai College, Patan, Maharashtra, India

Graphical Abstract

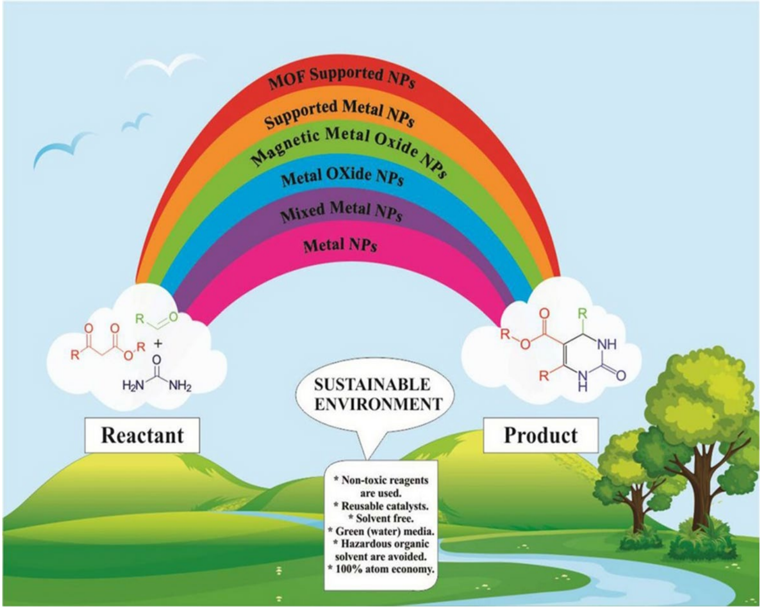

Keywords Nanocatalyst · Organic transformations · Green and sustainable chemistry

Introduction

The main principle of green and sustainable chemistry is to design the products and processes that minimize or eliminate the use of generation of hazardous substances [1]. Nanocatalyst is upcoming growing field and is acute fusion of sustainable technology and organic transformations; relevant to almost all types of catalytic organic transformations. Among nanocatalyst, several forms such as magnetic nanocatalysts, metal nanocatalysts, metal oxide nanocatalysts, nano mixed metal oxide, core–shell nanocatalysts, nano-supported catalysts, grapheme oxide-based nanocatalysts, have been selected in catalytic applications [2]. The area of benign organic synthesis a broad array of nanostructured catalysts have been used especially, transition metal oxide nanocatalysts are promising material for organic transformations. Nanocatalyst found to capture the best catalytic role compared to that of conventional catalyst due to their dominant catalytic activity, selectivity and durability can be achieved by their small size (1–100 nm), shape, composition, and nature of nanocatalyst structure. These observable benefits of nanocatalysts are depending on the nanosize effect; catalytic property; generally increases with decreasing size of nanocatalysts [2]. The component of green solvents and charming nanocatalysts seems to be an effective way to develop the newer generation of green and sustainable protocols.

The tuning of important organic transformations has latterly enveloped various innovative scientific developments accomplished by improved and attractive synthetic practices that avoid the use of hazardous reagents and reactants [3]. Till the date nanostructured materials are plays a crucial role in various types of organic transformations including multicomponent reactions, chemo-selective oxidations, hydrogen transfer reactions, oxidative aminations, coupling reactions, asymmetric hydrogenations, oxidative esterifications, C–H activations, hetrocyclic reactions, C–C bond formation reactions, and more. Also, nanoscale materials find use in a variety of different sectors; such as electronic, magnetic, solar cell, sensors, biomedical, pharmaceutical, energy, environment [4]. Due to the notable strength of this technology, there has been a worldwide increase in investment in nanocatalysts research and development. Main focus on sustainable development has been made using these nanocatalysts in terms of diversity of the organic reactions, activity, selectivity and reusability [5]. For sustainable organic transformations, it not only includes green way of synthesis but also considers the cost analysis of nanoacatalysts for several reasons that, sustainability, energy efficiency, resource conservation, catalyst recycling, affordability, large-scale production, research advancement, commercial viability. The importance of cost-effective nanocatalysts lies in their potential to make, catalytic processes economically feasible, sustainable, and widespread. Investing in the development and application of affordable nanocatalysts can have significant positive impacts on both the economy and environment. In conclusion, it is believed that we try to provide the design and development of well-defined advanced multifunctional especially, transition metal oxides nanomaterials and imperative sustainable protocols for decoration of catalytic organic transformations in greener medium, and other various applications such as gas sensing, solar cell, and biological screening which will satisfy many criteria of "Green Chemistry" (Fig. 1).

Nanoparticles synthesis methods

The two general approaches that are generally used for the fabrication of nanoparticles are “top-down” and “bottom-up” approach according to the processes involved in preparing nanoscale structures. The “top-down” approach involves the thermal, chemical, or mechanical disintegration of large particles of bulk metal into nanoparticles, while the more common “bottom-up” approach involves the creation of metal from the reduction or decomposition of a precursor first followed by the agglomeration of the metal to produce the nanoparticles [6]. Now a days, transition metal oxide are intensely studied due to their unique optical, electrical, and catalytic properties such as low preparation costs, excellent activity, great selectivity, efficient recovery and good recyclability compared to bulk materials (Figs. 2 and 3).

Fig. 1 Progression of green chemistry principles over environment deflation

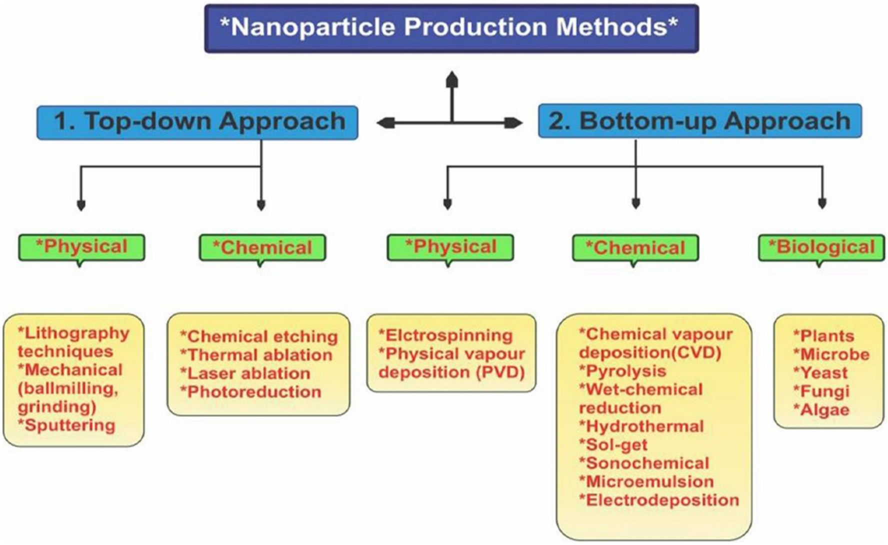

Fig. 2 Fabrication of nanoparticles using "Top-down" and "Bottom-up" techniques

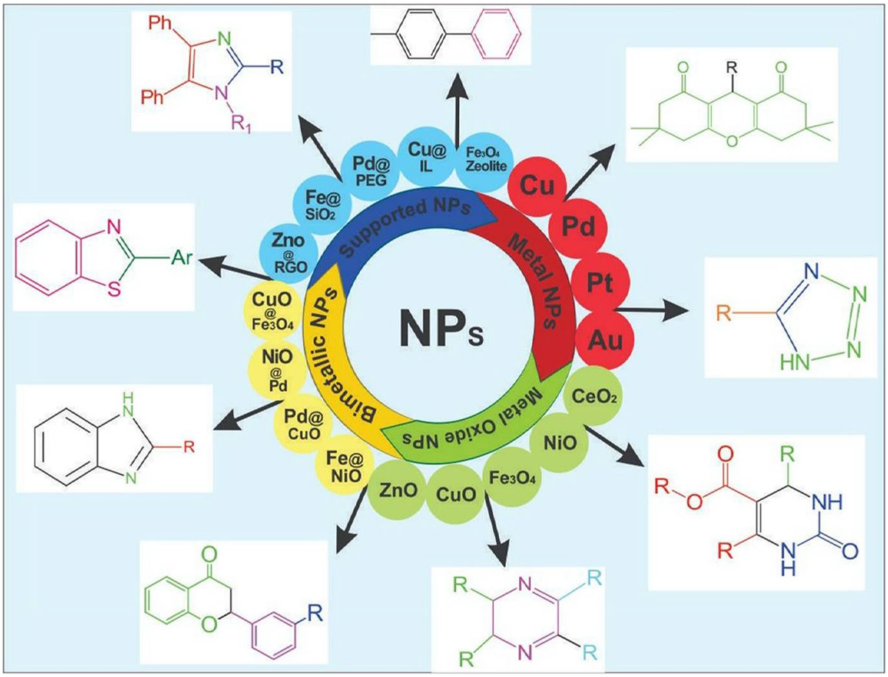

Fig. 3 Catalytic applications of NPs for various organic transformations

Metal NPs

The last tenner has validated enormous production of metal nanoparticles in the field of nanocatalyst. Metal NPs are synthesized from metals to nanomeric sizes almost all the metals can be synthesized into their nanoparticles [7]. Multiple records have shown their incredible level of achievement as a catalyst in terms of selectivity, reactivity, and product yield [8].Transition metal NPs have arrived great interest because of their brilliant properties like longevity, enormous surface area, and high reusability as catalyst [9]. The commonly used noble metals for nanoparticles synthesis are Copper (Cu), Palladium (Pd), Gold (Au), Platinum (Pt), etc., have gathered the attention from researchers, for their usage in organic transformations includes different multicomponent reactions, heterocyclic reactions, hydrogenation reactions, oxidation reactions, couplings reactions, enabling the formation of C–C and carbon heteroatoms (C–N, C–O) bonds, reduction reactions, catalytic dehydration and dehydrogenation reactions, amination, C–C bond formation reactions, hydroamiantion reactions with a wide range of elctrophiles that could lead the synthesis of industrial important compounds with various functional groups. Also, exploited for a number of advanced functional applications such as sensors in electronic devices [10], and catalysis [11].

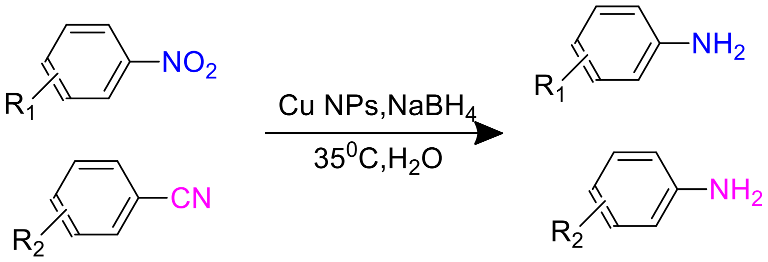

Scheme 1 Reduction in nitroarenes and benzonitriles

Copper (Cu) NPs

Zamani et al. and Ansari et al. generated a new protocol for reduction in nitroarenes and benzonitriles (Scheme 1) in green aqueous medium by using Cu NPs [12].

Palladium (Pd) NPs

For more than three decades, Pd NPs has been successfully occupied in the synthesis of C–C bonds. Near about all types of C–C coupling reactions in important organic transformations such as Heck, Suzuki, Sonogashira, Negishi and Stille are reported by Pd NPs [13]. The extraordinary nature of the Pd NPs as catalyst in this task is due to many constituent like low catalyst loading and recyclability. Qiu et al. synthesized Suzuki-Miyaura coupling (Scheme 2). Pd NPs dimensions vary between 8 and 30 nm were used as a catalyst, structural composition, external morphology, particle size distribution, of Pd NPs were confirmed by various characterization techniques such as SEM, TEM, HR-TEM, XRD, XPS for confirmation of oxidation state of Pd nanocatalyst [14]. Sawoo et al. studied Pd NPs catalyzed Sonogashira (C–C) coupling reaction (Scheme 3). Authors did the

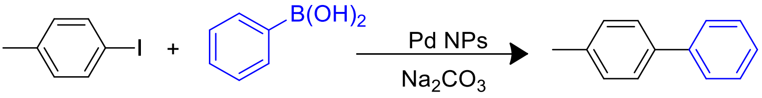

Scheme 2 Suzuki–Miyaura reaction

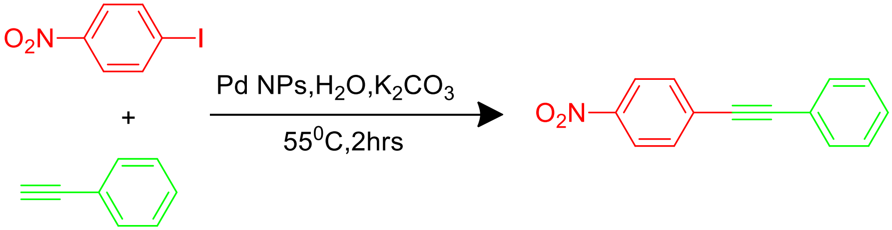

Scheme 3 Sonogashira coupling reaction

purification of isolated product yield by flash colum chromatoghraphy by using petroleum ether or ethyl acetate as a eluent [15].

Gold (Au) NPs

Gold NPs, attracted the marketplace from researchers because they have a unique identity; as steady and biocatalyst. Therefore, they gathered a significant place in the field of catalysis for sustainable organic synthesis. Au NPs shows superb properties in both oxidation and reduction reactions. Nitroaryl compounds are used as an organic contaminants in farming and manufacturing wastewater and many others fields. Therefore, the important chemical transformations; that is reduction in nitroarenes is usually studied. Guo et al. reported, water soluble Au NPs steadied by PEG and used as catalyst for the selective reduction in nitroarene (Scheme 4). In addition, authors also carried out evaluation of the gold nanoparticles size about 3 nm and used as a refractive index sensor [16].

Platinum (Pt) Nps

Platinum NPs, is nobel and immoderate metal, Pt NPs and nanowires capture extra courtesy headed for their various applicatives in solar cells and fuel cells. In organic transformations Pt NPs acting best character as a catalyst in hydrogenation and oxidation of organic compound as compared to bulk Pt. Recently, Saha et al. testified, selective oxidation of alkylarenes to aromatic acids/ketone (Scheme 5) in water catalyzed by using decomposable binapthyl stabilized Pt NPs [17]. Key function of this protocol is, the aqueous tert-butyl hydroperoxide (TBHP) as a greener oxidant and water as a green solvent have been used in this oxidation reaction. The analytical studies of the synthesized Pt-BNPs was evaluated through FT-IR, UV–Visible, XRD techniques. Author also conducted the hot centrifugation for separation of catalyst from reaction medium and mercury poisoning test to prove that Pt-BNP catalyst is

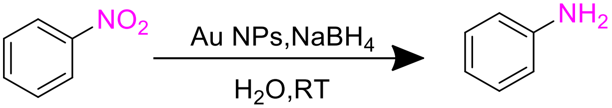

Scheme 4 Reduction in *p*-nitrobenzene to aniline

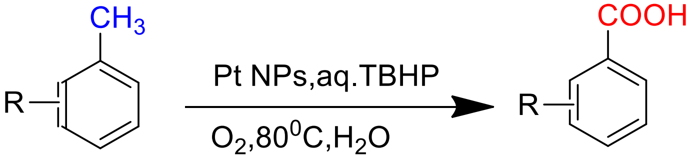

Scheme 5 Selective oxidation of alkylarenes to aromatic acids/ketone

heterogeneous and not the leached in solvent. Authors claimed that, Pt-BNPs can be recovered and use again up to sixth series devoid of far beating in its catalytic performance. In ongoing efforts there are needs to substitute the noxious reducing agents with naturally-safe benevolent protocol, which can acts as both reducing agent as well as stabilizing agents. The prior selection of stabilizers is also furthermost essential to avoid the self-aggregation of metal NPs. Because the self-aggregation of metal NPs affects on stability, catalytic activity, and overall recyclability of metal Nps in the catalytic system (Table 1).

Transition metal oxide NPs

The last decade has validated enormous production of metal oxide nanoparticles in the field of nanocatalysts, Transition Metal oxide NPs illustrated excellent properties that make them assuring materials for application as nanocatalysts [24]. Near about all the metals can be synthesized into their nanoparticles. Several reports have shown their noticeable level of performance as a catalyst in terms of selectivity, reactivity, and product yield [8]. Synthesis of nanoscale transition metal oxides such as zinc oxide, copper oxide, tin oxide, titanium oxide, iron oxide, nickel oxide, cerium oxide, zirconium oxide, and cobalt oxide have a convincing attraction as sustainable nanocatalysts. Metal oxide NPs are also used in the industrial field due to their unique role in various fields such as transistors, UV detectors [25], solar cells, sensors [26], gas sensing [27], antibacterial agents [28], catalysis. There are many methods described for the synthesis of metal oxide NPs such as, microwave technology [29], ball-milling, ultrasonication [30], hydrothermal [31], sol–gel [32]. Notable development has been made using these metal oxide nanocatalysts (transitions and inner-transitions metal) toward organic transformations such as catalytic oxidations, photocatalysis, hydrogenation, coupling reactions, C–C bond cleavage reactions, dehydogenaton reactions, heterocyclic reactions due to their distinctive properties such as; low preparation cost, excellent activity, great selectivity, high stability, efficient recovery, and good recyclability.

Zinc oxide NPs

Zinc oxide nanoparticles are prominent nanomaterials due to their sustainable nature and significant properties such as, low preparation cost, eco-friendly nature, reusable, high reactivity, and stability. Recently, Attar et al. successfully prepared zinc oxide NPs by chemical co-precipitation method as well as plant extract co-precipitation (biological) method in which *'Azadirachta indica'* leaf extract used as a capping agent. Analysis of synthesized ZnO NPs carriedout by various characterization techniques such as FT-IR, TGA-DTA, XRD, BET, SEM, and EDX. Authors observed that, ZnO-PE have noteworthy large BET surface area and pore volume compared to ZnO-CM; these are 58.862 m^2g^{-1} and 8.1624 m^2g^{-1} and 0.6897 cm^3g^{-1} and 0.1349cm^3g^{-1}, respectively. These results prove that the adsorption capacity of ZnO-PE will be greater than that of ZnO-CM. The average pore size of ZnO-PE (46 nm)

Table 1 Metal NPs for organic transformations

Sr No	Metal NPs	Condition	Features	Yield %	NPs Size (nm)	TOF h^{-1}	References
1	Cu NPs	$NaBH_4/H_2O$,35 °C	Rea^n of nitroarnes and benzonitriles	99	15–22	–	[12]
2	Pd NPs	Na_2CO_3	Suzuki–Miyaura coupling	99	1.8–0.2	–	[14]
3	Pd NPs	K_2CO_3, H_2O, 55 °C,2 h	Sonogashira coupling rea^n	96	10	–	[15]
4	Au NPs	$NaBH_4$, rt, H_2O, 1 h	Nitroarene reduction	99	1.1	–	[16]
5	Pt NPs	TBHP, O_2, H_2O, 80 °C	Oxid^n of alkylarenes to aromatic acids	79–95	5–8	–	[17]
6	Cu NPs	Solvent-free	Ulman reaction for biphenyl	92	40–80	–	[18]
7	Cu NPs	70°c, 65–70 min	Synthesis of chromene derivatives	95	50	–	[18]
8	Cu NPs	100 °C, 7–8 h	Hydrogenation of azides	83	6–8	–	[19]
9	Cu NPs	H_2O,70 °C,1–7 h	Click reaction	50–98	~3	–	[20]
10	CO NPs	TBAA, TBAB, 120 °C, 45 min	Heck reaction	90	–	–	[21]
11	Ag NPs	THF/H_20, 3 h, 100 °C	Hydrogenation reaction	60	–	–	[22]
12	Ag/CNT	EtOH	Sonication of anthranilamides and aldehydes	80	30	–	[22]
13	Au NPs	H_2O, TFE, 40 °C	A^3 Coupling MCR	70–90	20	–	[23]

is smaller than ZnO-CM (66 nm). Smaller pore size and high surface area due to this uniqueness ZnO-PE NPs show good catalytic performance in the synthesis of benzylidenemalonitrile (BMN) (Scheme 6) and tetraketone (Scheme 7) in an aqueous hydrotropic medium at room temperature [33]. Chromatographic free separation, very low reaction time, high yield, and reusable catalyst, and green reaction media due to this strong arms this protocol become very advantageous and eco-friendly.

In another report, Hassanpour et al. well synthesized ZnO NPs as an effective catalyst for the synthesis of dihydropyrimidones (Scheme 8) in high yield via a one-pot three component reaction in water. After completion of reaction, the catalyst was recovered and reused successfully without any significant loss in their catalytic activity. Dihydropyrimidone possess significant biological efficiency that include antiviral, antibacterial, antihypertensive and antitumor activity [34].

Shinde et al. studied ZnO catalyzed synthesis of flavanone (Scheme 9) in the presence of water at room temperature [35]. ZnO NPs was eliminated from reaction mixture by simple centrifugation method. In present protocol authors observed that catalyst can be recycled at least five times without any change in its activity.

In another report, Paul et al. studied the biological active 2-substituted benzimidazoles (Scheme 10), catalyzed by ZnO NPs under biogenic pathways from the seed

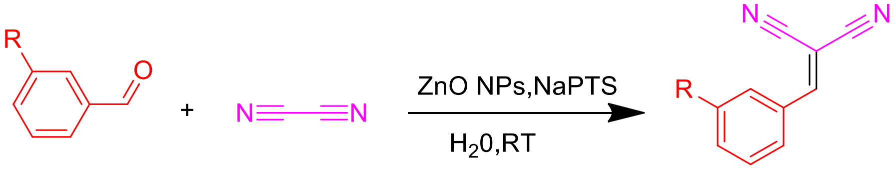

Scheme 6 Synthesis of benzylidenemalonitrile

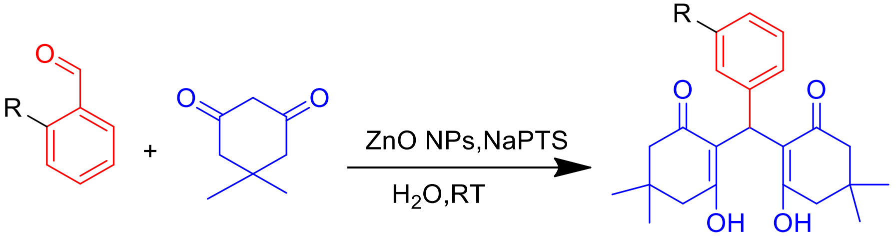

Scheme 7 Synthesis of tetraketone

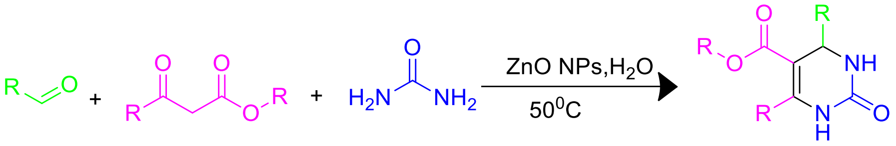

Scheme 8 Synthesis of dihydropyrimidones

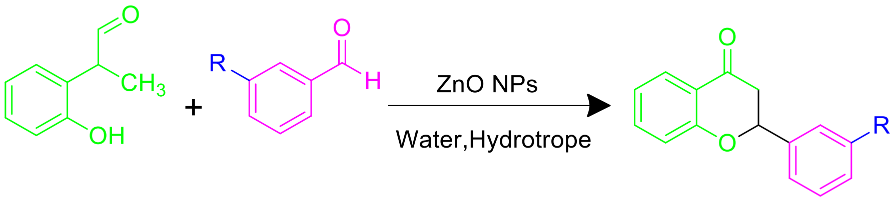

Scheme 9 Synthesis of flavanone

Scheme 10 Synthesis of 2-substituted benzimidazoles

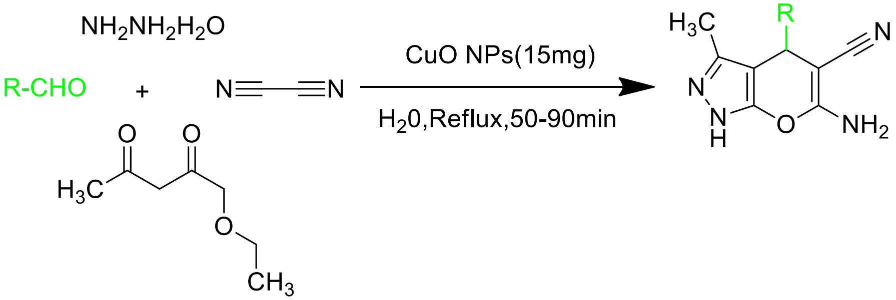

Scheme 11 Syntheis of pyrano[2,3-c]pyrazoles

extract of '*Parkia roxburghii'*.Ultrasonic irradiation in ethanol at room temperature [36].

Copper oxide NPs

Copper oxide nanoparticles has attracted more attention due to its miscellaneous properties and applications in numerous fields; CuO NPs have been extensively used as a catalyst because of their twofold nature that is Lewis acid and Lewis base and highly reactive large surface area. In recently, M. Shojaie et al. determined one-pot multicomponent synthesis of pyrano[2,3-c]pyrazoles (Scheme 11) catalyzed by CuO NPs as an efficient reusable catalyst has been developed. Authors analyzed CuO NPs could be reused at least seven times without a significant minimization in its activity [37].

Recently, Xia et al. studied; CuO NPs catalyzed synthesis of 1,3/1,4-diketones (Scheme 12) in aqeous medium from three component reaction of aldehyde,1,3-dicarbonyl compound and organic boronic acid [38]. In this report, CuO NPs (with size near about 40 nm) were directly takes from distributors (Aladdin, 99.9%

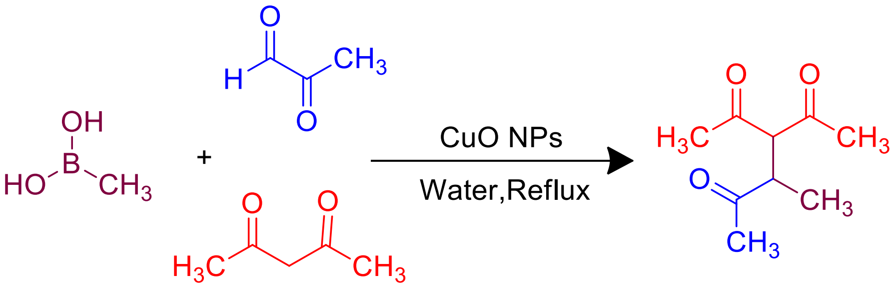

Scheme 12 Synthesis of 1,3/1,4-diketones

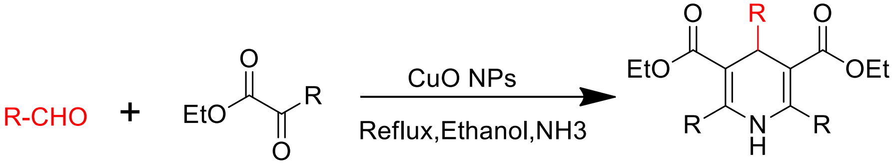

Scheme 13 Synthesis of pyridine derivatives catalyzed by biogenic CuO NPs

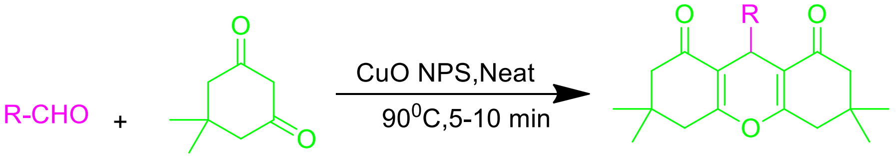

Scheme 14 Synthesis of 1,8-dioxo-octahydro-xanthenes

metals). This method has many positive sides, such as a convenient reaction setup, ignoring the use of hazardous organic solvents, broad substrate demand, and gram-scale synthesis.

Javad. S. Ghomi et al. [39], synthesized pyridines derivatives (Scheme 13) catalyzed by biosynthesized CuO NPs. This protocols reports a lot superiority such as easy handling operation, wide range of products, excellent yields, minimum reaction time, repairable of the catalyst, and low catalyst loading.

Xanthenes, in certain, 1,8-dioxo-octahydroxanthene constituent, have attributed special consideration due to their best pharmacological properties such as, anticancer antimicrobial, and enzyme inhibitory activity. On the other hand, Safaei-Ghomi et al. have investigated xanthene derivatives (Scheme 14) using CuO NPs as catalyst. Lately, they stated an easy approach for the efficient synthesis of 1,8-dioxo-octahydroxanthene moieties via a one-pot pseudo 3C condensation between various aldehydes and dimedone in the presence of CuO NPs under solvent-free techniques [40]. Last decades has seen tremendous advantages of CuO NPs as a mild, inexpensive, effectual, environmentally-safe, harmless, long-lasting catalyst for various organic transformations.

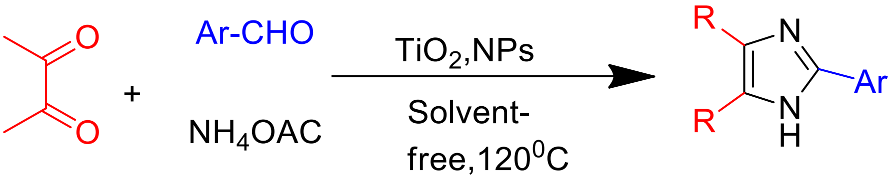

Scheme 15 Synthesis of 2,4,5-triarylimidazoles by TiO_2 NPs

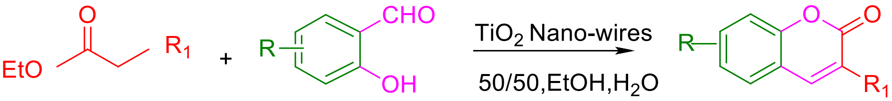

Scheme 16 Synthesis of coumarin derivatives

Titanium oxide (TiO_2) NPs

Currently, titanium oxide NPs have raised as an captivating multifunctional material. TiO_2 NPs have marvelous properties such as high stability, durability, non-toxic, and broad-spectrum, antibiosis, distinctive morphologies (size, shape, and texture) and surface chemistry. Nano TiO_2 NPs has been verified to be an magnificent catalyst in synthetic chemistry as its depicts extraordinary activity, non-hazardous nature, easy availability, renewability, strong oxidizing agent, Lewis acidity, and long lasting. As well as TiO_2 NPs have been used as a green catalyst in many organic reactions, photocatalysis reactions [41]. On the other hand, Lee Eng Oi et al. studied solvent-free synthesis of quinazolinone, in this TiO_2 NPS were used as a catalyst [42]. Latterly, Fedorova et al. reported, synthesis of 2,4,5-triaryl imidazoles (Scheme 15) biological active compound in presence of commercially available TiO_2 NPs. Heating mixture of these reagents in the absence of solvent gave better yield of the target products. The potential of catalyst determined only insignificantly after five runs of reuse [43]. Also, Kumar and his group employed TiO_2 NPs, nanowires as an efficient, reusable catalyst for the one-pot green synthesis of coumarin derivatives (Scheme 16), in ethanol/water solvent system under reflux condition. Coumarins are very common in the naturally occurring heterocycles illustrated deep scope in pharmaceutical industry [44].

Nickel oxide (NiO) NPS

In recent time, NiO NPs are attracting a great deal of attention as a catalyst in terms of some key strength such as selectivity, reactivity, and improved yield of products, for hydrogenation reactions and various organic transformations. B. Reddy and team studied synthesis of quinolines derivatives (Scheme 17) by

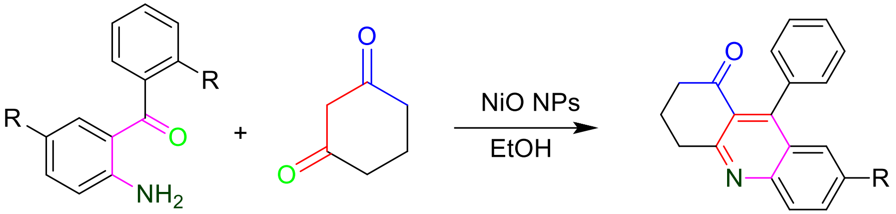

Scheme 17 Synthesis of quinolines

using NiO NPs (30 nm) ethanol medium [45]. Size and morphological studies of synthesized NiO NPs were categorized by XRD and TEM. The said protocol is beneficial owing to its simple operating, comparatively short reaction time, often good to high average yields, favorable workability, and ecological friendliness.

Magnetically separable Fe_3O_4 NPs

Fe_3O_4 NPs are plausibly the most extensively studied the main property of these nanoparticles is the easy and convenient separation from reaction media by using external magnet. Recently magnetite nanoparticles were used as an highly efficient catalyst in many organic transformations. Zhan-Hui Zhang and his group interpret the synthesis of magnetic nanocatalyst and its applications in multicomponent reactions [46]. L. M. Ross et al. produced xanthene derivatives by using magnetic separable Fe_2O_3 NPs as a catalyst [47]. XRD studies of Fe_2O_3NPs firmed that the resultant nanoparticles were spherical in shape with about 20 nm size. Fe_3O_4 NPs act as best Lewis acids role due to that 3*d* orbital of the Fe interrelates with the carbonyl group. In conclusion, authors claimed that, catalyst can be healed and reutilized many counts without any except deficit in its action. Reuben Hudson and Rajender S. Varma and co-workers demonstrate the magnetic nanoparticles serve the dual role of a catalyst and a magnetically recovery entity. Authors observed that the Iron oxide Nps are robust, stable in atmosphere, obedient to functionalization, suspendable in many solvents including water or protic benign solvents; their size, shape, and crystallinity can be finely tuned. Authors studied the catalytic advantages of iron oxide NPs in oxidative reactions, C–H activations, and oxidative coupling reactions, therefore, the catalytic demand of magnetic NPs increased. Spinel structure that is mixed spinel, doped spinel, and three component spinels have been intensely studied and their catalytic activity have been evaluated for CO_2 reduction, water splitting, methanol decomposition. After completion of reaction, the catalyst were simply removed by using a magnet. The recovered MNPs were washed and reused for the next cycle [48]. In another report, "*chlorophytum comosum'*" aqueous leaf extract was utilized for the biogenic synthesis of iron oxide nanoparticles with a size of 50 nm confirmed by XRD, TEM and tested against *P. aeruginosa, E. faecalis, E. coli, and S. aureus.* On the one hand, Fedrova et al. reported magnetic iron oxide NPs used as modest and reformable catalyst for the four-component Hantzsch reaction (Scheme 18**),** condensation of dimedone, alkyl acetoacetate, and ammonium

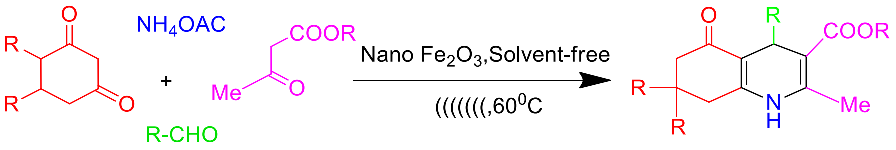

Scheme 18 Synthesis of pyridines by nano Fe_2O_3

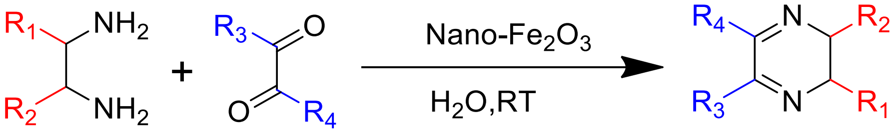

Scheme 19 Synthesis of tetra-alkylpyrazine

acetate with various aldehydes under solvent-free conditions and ultrasound irradiation at 60 °C temperature [49]. Also, they carried out synthesis of tetra-alkylpyrazine (Scheme 19).

In another study, Safari and his group described chitosan functionalized Fe_3O_4 NPs was used for one-pot synthesis of 2-amino-4*H*-chromenes. The MNCs was designed to produce a 99% yield of the target product under ultrasound assisted in a short time, furthermore the authors claimed that the catalyst were recycled using a magnet and reused five times without remarkably significant loss in its activity but only 2% yield was reduced in fourth cycle [50]. The reutilization of the catalyst is very important for large-scale operations and an industrial point of view. These nanoparticles offers several rewards counting relaxed workup process, excellent profit and reproducibility of the catalyst lacking addition of its catalytic activity. These catalyst demonstrate magnetic recuperability, which reduces the need of catalyst separation later finishing point of the reaction but suffer from some drawbacks i.e. requirement of a complicated and vapid operation for their synthesis. Lately, R. Gurav and his team scrutinized the novel one-pot MCR of tosylate, aryl aldehyde, and thiosemicarabazide for the synthesis of hydrazinyl thiazoles (Scheme 20) using Fe_2O_3 NPs derives from rusted iron as a catalyst. The size and morphology (20–100 nm, crystalline nature) of the Fe_2O_3 NPs were evaluate by HR-TEM. The magnetic Fe_2O_3 NPs were easily regained from the reaction using an external magnet and the catalytic study of reduced catalyst was examined over four cycles. Further, the authors were carried out analysis of synthesized molecules for their medicinal activity, which further supported through molecular docking [51].

Zirconium oxide (ZrO_2) and Cerium oxide (CeO_2)

Metal oxide nanoparticles of the second transition series also exhibit an central part in organic transformations because, of their advanced properties of large and reactive surface area, simple task for preparation and isolation, low expense,

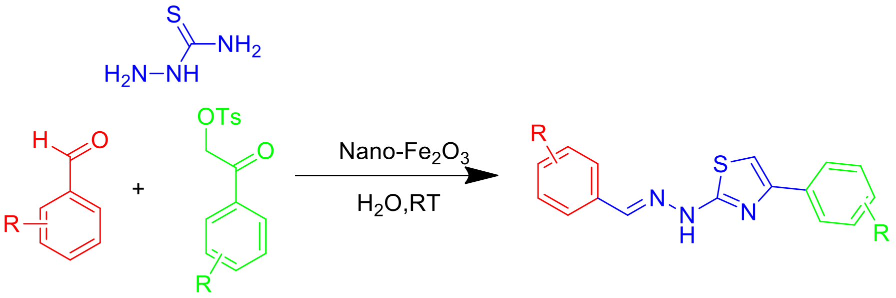

Scheme 20 Synthesis of hydrazinyl thiazoles

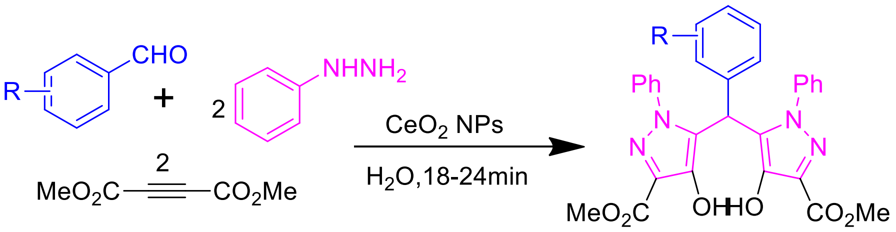

Scheme 21 Synthesis of C-tethered bispyrazole-5-ols derivatives

high recovery rate, reusability and green properties, therefore, a lot of interest in numerous chemical transformations using catalysts has been increased [52]. Cerium oxide and zirconium oxide are a dominant material for different kinds of industrial applications related to catalysis, the tiny size and large specific surface area of nano-sized CeO_2 allow for certain fixed and unusual physicochemical properties [53]. Safaei-Ghomi and co-workers have explained multicomponent synthesis of C-tethered bispyrazol-5-ols using CeO_2 NPS. In addition a synthesized bispyrazole derivatives (Scheme 21) shows efficient biological activities such as antioxidant and antibacterial activity. This protocol become well workable due to its decent properties like high yield, milder reaction state and green catalyst [54].

Saha et al. explained fluorescent tetragonal ZrO_2 NPs catalyzed multicomponent synthesis of pyrano[3,2-c] chromene derivatives (Scheme 22**).** Authors derived that ZrO_2 NPS produced higher catalytic activity even at 10th cycle. A couple of reaction time, easy workup procedure, wide substrate tolerance, small catalyst loading, high yield of product, and solvent-free conditions, etc., are some of the main attribution of these developed protocols [55].

Cobalt oxide (CO_3O_4) NPs

Cobalt oxide nanoparticles are traditional transition metal oxide and have magnetic *p*-type semiconductors and interesting catalytic properties; as well as other unique applications in various different areas such as photocatalytic, antimicrobial, activity

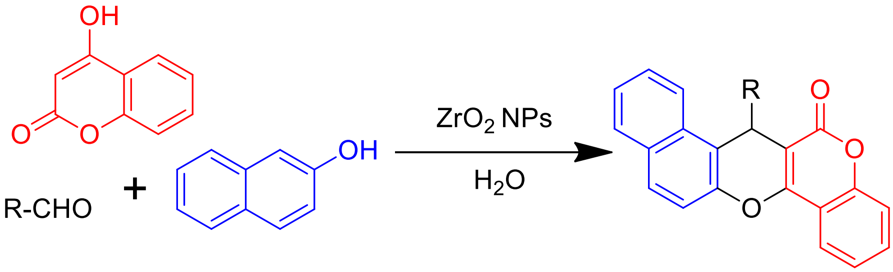

Scheme 22 Synthesis of chromene derivatives

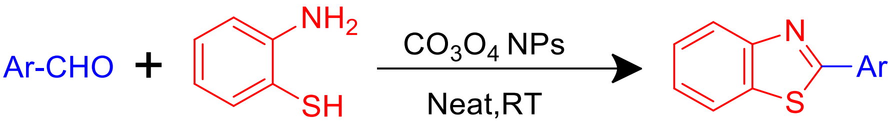

Scheme 23 Synthesis of benzothiazole derivatives

and electrochemical sensing. S. Z. Mohammadi and group reports, "*walnut green'*" plant extract based green synthesis of cobalt nanoparticles (60 nm, spherical). Authors study explains the plant extracts plays important role because they contains various key phytochemicals such as phenols, alkaloids, terpenoids, and various vitamins. These phytochemicals acts as reducing, capping, and stabilizing agent. Further the advantages of cobalt nanoparticles in photocatalytic, electrochemical sensing, and antibacterial applications [56]. Geetika Patel et al. synthesized benzathiazole derivatives (Scheme 23) using CO_3O_4 NPs (nano-flake) as a reusable catalyst. The crystal-clear structure and morphology and elemental mapping of Co_3O_4 NPs have been analyzed by different analytical techniques such as, UV–Vis, fluorescence, powder X-ray diffraction, FE-SEM, and EDX. Authors observed that; catalyst were reused for at least ten times without appreciable loss of catalytic activity [57]. P. G. Kargar and G. Bagherzade are derived synthesis of poly-substituted piperidine derivatives (Scheme 24) by using cobalt oxide as a green trinuclear catalyst. CO_3O_4 NPs has three strong arms that is highly efficient, biodegradability and easily available catalyst with simple and clean profile, and extensive yields, and very short reaction time, besides the safe solvent ethanol, simple purification and recrystallization of products, provides a good example of a competitive and alternative synthetic methodology [58].

Vanadium oxide NPs

In recent time, V_2O_5 NPs gained a special devotion due to their cost-effective and harmless nature. In addition V_2O_5 NPs have worthy reactivity and selectivity for various organic transformations. Prof. M. Paramasivam and group synthesized biological active pyrazole napthoquinone derivatives (Scheme 25). In presence of V_2O_5

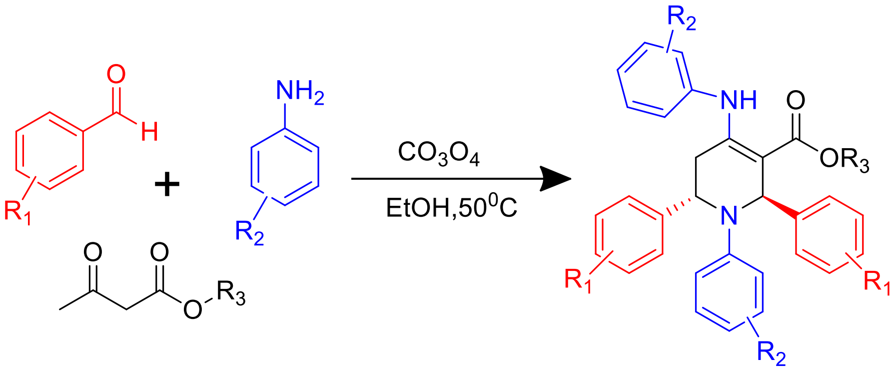

Scheme 24 Synthesis of piperidine derivatives

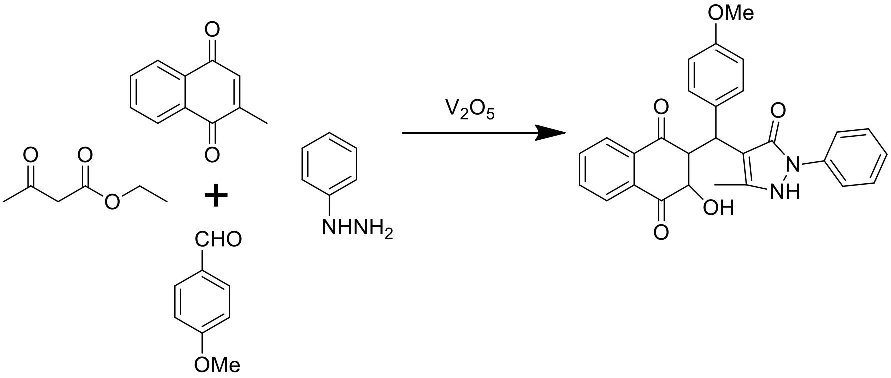

Scheme 25 Synthesis of pyrazole napthoquinone derivatives

NPs using green solvent such as ethanol.V_2O_5 NPs acts as best catalyst due to its three strong arms that, low cost, more abundant, easy to handle catalyst. Furthermore, authors analyzed the synthesized compound have been employed for their biological screening in vitro anticancer activity against cervical cancer cell line (Hela). Also, authors examined that, this method delivers an excellent atom economy (100%) and carbon efficiency with notable economic and eco-friendly returns [59].

The use of metal oxide catalysts in organic synthesis and other various fields has significantly enhanced, due to their stability and tunable properties due to this nature it has become great challenging for nanotechnology world (Table 2).

Table 2 Metal oxide NPs for organic transformations

Sr No	Metal Oxide NPs	Condition	Features	Yield (%)	NPs Size (nm)	TOF h^{-1}	References
1	ZnO NPs (10 mol%)	NaPTS, H_2O rt, 5–10 min	Tetraketone and Benzylidene- malonitrile derivatives	85–95	45–65	114s	[33]
2	ZnO NPs (4 mol%)	H_2O, 50 °C	Synthesis of Dihydropyrimidone (Biginelli reaction)	75–98	50–70	–	[34]
3	ZnO NPs (5 mol%)	Hydrotope rt, H_2O	Synthesis of Flavanone	92–96	~90	–	[35]
4	ZnO NPs (0.5 mol%)	EtOH, 10 min	Synthesis of 2-substituted benzimidazoles	96	30	–	[36]
5	ZnO NPs (0.5 mg)	EtOH, rt, 10 min	Synthesis of pyridines/ pyrimidines	90	–	–	[37]
6	CuO NPs (15 mg)	Water, Reflux, 30–90 min	Synthesis of pyrano/ pyrazoles derivatives	88–98	40	–	[37]
7	CuO NPs	H_2O, reflux	Synthesis of 1,4-diketones	87	40	–	[38]
8	CuO NPs	Ethanol, NH_3, Reflux	Pyrimidine derivatives	80	90	–	[39]
9	CuO NPs (12 mol%)	Solvent-free, Neat, 90 °C 5–10 min	Synthesis of 1,8-dioxooctahydroxanthene	80–97	40	–	[40]
10	CuO NPs (10 mol%)	$NaBH_4$ H_2O, rt	Reduction in P-nitrophenol	94	30–40	–	[41]
11	Tio_2 NPs	Solvent-free	Synthesis of triaryl imidazoles	93	–	–	[43]
12	Tio_2 NPs	50/50 EtOH/H_2O	Synthesis of Coumarin	85	–	–	[44]
13	Nio NPs	EtOH	Synthesis of Quinolines	80	–	–	[45]
14	Fe_2O_3 NPs	H_2O, rt	Synthesis of tetraalkyl pyrazine	90	18	–	[49]
15	Fe_2O_3 NPs	H_2O, rt	Synthesis of Hydrazinyl thiazoles	95	20	–	[51]
16	CeO_2 NPs	H_2O, 70 °C	Synthesis of C-tethered bispyrazoles	86	11	–	[54]
17	ZrO2 NPs	H_2O, 80 °C	Synthesis of Chromene derivatives	88–94	12	–	[55]
18	CO_3O_4 NPs	Neat, rt	Synthesis of Benzothiazole	87–97	–	–	[57]

Table 2 (continued)

Sr No	Metal Oxide NPs	Condition	Features	Yield (%)	NPs Size (nm)	TOF h^{-1}	References
19	CO_3O_4 NPs	EtOH, 50 °C	Synthesis of piperidine derivatives	92	10	–	[58]
20	V_2O_5 NPs	Ethanol	Synthesis of pyrazole napthoquinone	85	30	–	[59]
21	ZnO NPs	H_2O, rt	Synthesis of pyrazole napthoquinone	90	< 50	–	[60]
22	CuO NPs	Reflux, EtOH:H_2O	Furan derivatives	75–91	10	–	[61]
23	CeO2 NPs	H_2O	Synthesis of spiro-oxindole	93	–	–	[62]

Bimetallic NPs

Bimetallic nanoparticles is a fusion of two different metals that reveals novel and immensely upgraded properties like optical, catalytic, biological, etc. BMNPs performs superior catalytic activity than their monometallic correlative complements in many organic transformations [63]. Bimetallic NPs can be in the form of alloys, core–shell. Newly, BMNPs progressively captivating additional concentration due to their novel properties as they are extremely functional and applicative in numerous fields such as electronics, pharmaceutical and in catalyst because they are cheap, steady alternatives that exhibit high activity and selectivity. Hence, a lot of efforts has been put into the development of these catalysts [64]. The nanocatalyst in the form of Au/AlO_3, Au/Fe_2O_3, Ag/TiO_2, Au/ZnO, Au/SiO_2 are studied for organic reactions such as, hydrogenation, oxidation, and cross-coupling. Bhaduri et al. used recyclable Au/SiO_2-shell/Fe_3O_4-core for the reduction in nitroaromatic compounds. Maria and group reported synthesis of plant based bimetallic Ag/ZnO nanocomposite and its applicability toward catalysis as well as in the field of biosensors, photocatalytic use, drug delivery, medicine, etc., [65] and analyzed by XRD, AFM, SEM, and EDX spectral techniques.

Core–shell bimetallic NPs

Core–shell BMNPs, when a single metal core coated by another metal or metal oxide results the formation of core–shell nanoparticles. Core–shell bimetallic NPs owns brilliant catalytic activity than alloyed bimetallic nanoparticles [66, 67]. Nanoparticles production methods among that biological synthesis of NPs is one of the modest economical and green method. On other hand, Mishra et al. designated biofabrication of core–shell CuO–Pd NPs from '*cyperusrotundus rhizome extract'* and moreover, used as catalyst for various organic transformations [68]. The surface roughness of the nanoparticles analyzed by AFM. Furthermore, CuO–Pd nanocatalyst was separated by easy percolation and can be reprocessed up to fifth succession. Authors claimed that the catalytic efficiency and the XRD pattern and TEM images are unaffected subsequently the fifth turn due to this promising nature of core–shell CuO–Pd NPs catalyst can be used for comprehensive industrialized purposes.

Magnetically separable bimetallic NPs

Magnetically separable BMNPs, acquired considerable attentiveness due to its favorable nature as they are magnetically detached, recovered and deed as backing in bimetallic NPs. Nitro group reduction is one of the mostly utilized organic transformations carried out by using this type of catalysts. The magnetically separable NPs employed a C-S formation using cellulose derived Fe_3O_4@Pd NPs as a catalyst for selective sulfenylation of indole derivatives (Scheme 26) Li et al. [69]. The catalyst was reutilized five times to give a 90% yield of the product.

Saha et al. and team, prepared magnetically recoverable $CuFe_2O_3$ and used for the synthesis of chromeno [4,3-b]pyrrol-4(1*H*)-one derivatives (Scheme 27) in aqueous

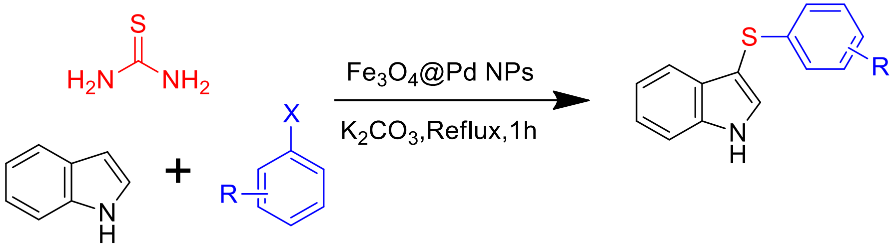

Scheme 26 Formation of indole derivatives

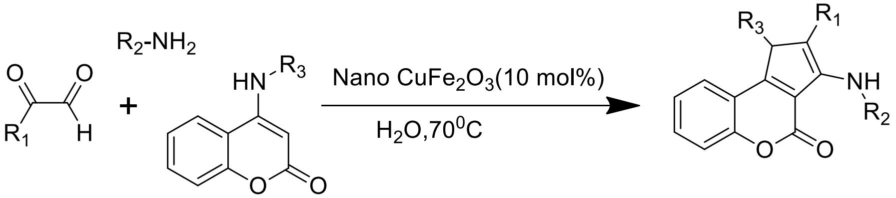

Scheme 27 Synthesis of chromeno[4,3-b]pyrorol-4(1*H*)-one derivatives

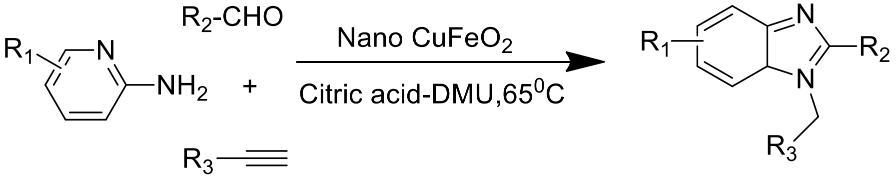

Scheme 28 Synthesis of imidazo[1,2-a]pyridines

media. They were prepared magnetic $CuFeO_2$ by using the sol–gel process and sequential annealing [70]. $CuFeO_2$ was found an efficient catalyst for the synthesis of one-pot, three-component reaction of imidazo[1,2-a]pyridines (Scheme 28) using citric acid-dimethyl urea melt as a green solvent. The catalyst was recycled and can be successfully reused six times without significant loss in its catalytic performance Lu J, Li XT et.al [71].

For developing more efficient and green chemical processes there are continued need and fully focused research on synthesis of magnetically recoverable multifunctional catalyst, due to their easy preparation process with high saturation, magnetization, lower toxicity, affordability and stability under vigorous reaction conditions.

Doped bimetallic NPs

Doped BMNPs, are also universally applicative in various fields such as; in catalysis, optical fiber, magnetic materials, battery cathodes, gas sensors, and in fuel cell because of their duel nature steadiness and electron transfer capability [72]. Biosynthesis of NiO and Fe doped NiO NPs by "*calotropisprocera'*" leaf extract, it

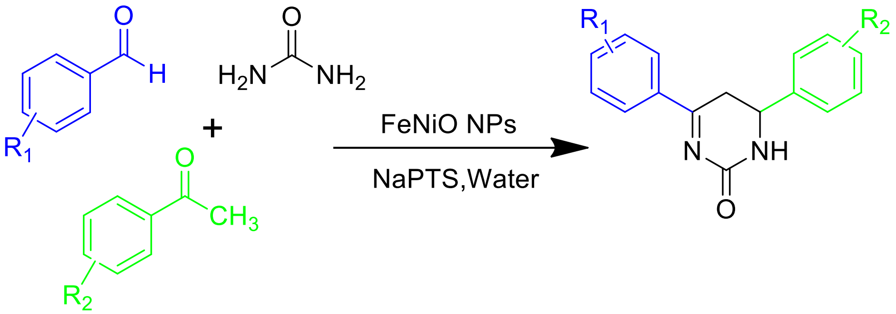

Scheme 29 Synthesis of diaryl pyrimidinones derivatives

performances as both reducing and capping agent and used as a catalyst for the synthesis of diaryl pyrimidinones derivatives synthesis in hydrotropic aqueous medium at room temperature (Scheme 29) Shinde and group. Also dopping of Fe^{+++} also gives disorderness in crystalline nature of Fe doped NiO. The effect of doping results in a decrease in particle size of Fe@Nio as compared to NiO NPs and catalyst shows superior performance in catalytic system. Conversely, authors detected healthier results for Fe@NiO for synthesis of pyrimidinones derivatives [73].

Now, eco-conscious days there is need to developing non-toxic biomaterials and eco-friendly reaction conditions, so scientists are obligatory to emphasis on improving a safer and a greener approach for organic transformations. Various metals like Cu, Mn, CO, Ni, rare earth and transition elements are used as dopant materials. The results of dopant material it decreases particle size in nm. Although, reduced size in nm enhance catalytic surface area, and ultimately shows good catalytic performance, nonetheless due to magnetic property it can be effortlessly parted, recycled and re-claimed with keeping its catalytic activity and also gives unprecedented ferromagnetic properties. Due to this multifunctional sides, these materials are not only used in organic transformations but also used in other areas such as for medical purposes in the antibacterial and anticancer therapy and drug delivery arena. The issues associated with the large-scale synthesis of metal-doped nanoparticles have yet to be explored for industrial also (Table 3).

Supported NPs

Supported nanoparticles receiving extensive attention and it play an important role as catalyst for a more green and sustainable society. When metal nanoparticles coated on top of the surface of nonporous material it result to form supporting metal nanoparticles, While formation of nanocatalyst particle size decreases to nanoscale dimensions due to which agglomeration of the particles into small clusters were formed. This agglomeration downgrades the catalytic strength. Toward reach the target of nanoparticles dimensions, shape, and efficiency it is needed to terminate agglomeration and partial growth, by adding of organic ligands, inorganic capping

Table 3 Bimetallic NPs for organic transformations

Sr No	Bimetallic NPs	Condition	Features	Yield (%)	NPs Size (nm)	TOF h^{-1}	References
1	Fe_3O_4@Pd NPs (10 mol%)	K_2Co_3, reflux 1 h	Formation of Indole derivatives	90	30	–	[69]
2	Nano $CuFe_2O_3$ (10 mol%)	H_2O, 70 °C	Synthesis of chromeno- pyrrol derivatives	80	50	–	[70]
3	Nano $CuFe_2O_3$ (10 mol%)	Citric-acid-DMU 65 °C	Synthesis of Imidazo pyridines	85	40	–	[71]
4	FeNiO NPs (5 mol%)	NaPTS, Water	Synthesis of diaryl pyri- midones derivatives	98	20–25	–	[73]
5	CuO-Pd BMNPs (2 mol%)	Reflux, H_2O, 30 min	Synthesis of 2,3-dihydroquinazolin-4(1H)-ones and spiro-oxindole	92–98	5	–	[68]
6	Ni@Pd BMNPs	H_2O	Cycloaddition of amines	95	10	–	[74]
7	Au–Pd BMNPs	DMF-H_2O, K_2CO_3 120 °C, 2 h	Sonogashira coupling of phenylacetylene and iodobenzene	96	10	–	[74]
8	Fe/Pd BMNPs	H_2O,rt, 12 h	Nitro group reduction	80–98	–	–	[75]
9	Cu@Fe BMNPs	H_2O,rt, 12 h	Azide-alkyne click reaction	93	–	–	[76]
10	$MnFe_2O_4$ BMNPs	H_2O, 90 °C	Synthesis of novel spiro-oxindole	78–82	33	–	[77]
11	Ni@ZnO BMNPs	H_2O, rt, NaPTS	Synthesis of 3,4-dihydropyrimidinone	84–96	80	–	[78]
12	Fe/Pd BMNPs	H_2O, 45 °C, 24 h	Suzuki–Miyaura cross-coupling	60–90	<50	–	[79]
13	$NiFe_2O_4$ BMNPs	–	Michael addition of active methylene comp	89–98	20	–	[80]
14	$CuFeO_4$ BMNPs	H_2O, 70 °C, 1-9 h	Synthesis of disustituted triazoles	74–86	–	–	[81]
15	$MnFe_2O_4$ (10 mol%)	H_2O, reflux, 2 h	Synthesis of novel spiro-furo pyrimidine-indolines	84–86	25–30	–	[82]

materials, metal salts, and polymer plays vital role [83]. The porous material is normally solid like silica gel [84], zeolites [85], metal oxides [86], activated charcoal [87], and graphite materials [88], carbon based material, magnetic materials, MOFs, naturally occurring clay and rocks [89], etc., used as porous suspension media. The use of supported metal NPs provides a much privileged results as compared to conventional homogeneous and heterogeneous catalysts for its catalytic performance as tuning reactivity, recyclability, high productivity and environment benevolent alternatives for organic transformations [90]. Supported NPs such as silica supported NPs, clay supported NPs, ionic-liquid supported NPs, graphene nanosheet (GNS) supported NPs, and metal organic frameworks (MOF) supported NPs are exhibit a broad area of applications due to their flourishing properties like surface reactivity, biocompatibility, stability, tunable pore size and high surface area [84]. Supported NPs are widely employed for hydrogenation of alkenes, alkynes and aromatic compounds, heterocyclic reactions, C–C coupling reactions, such as Suzuki–Miyaura, Heck, and Sonogashira reactions, C–C bond formation reactions like the Ulman reaction and C–H activation.

Silica supported NPs

Silica supported NPs, displayed a vast scope of utilization in many research-based areas, pharmaceutical field such as diagnostic tools and drug delivery. [84]. Kamali and Shirini detailed a magnetically recoverable $Fe_3O_4@SiO_2\text{-}ZrCl_2$ catalyst for the synthesis of tetra-hydrobenzimidazo[2,1-b]quinazolin-1(2*H*)-one derivatives (Scheme 30) under solvent-free conditions. Authors claimed that, there is no need to extra filtration of catalyst after completion of reaction because the catalyst was magnetically separable. [91].

Lately, V. Kamble et al. reported nano-silica sulfuric acid (Nano-SSA) catalyzed an effortless synthesis of azothiadiazoles via diazo coupling reaction of anilines with substituted amino thiazoles (Scheme 31) under co-grinding and solvent-free technique for economic and ecological point of view. In this regard, author synthesized nano-silica from raw material '*rice husk ash*' (RHA) and further supported with sulfuric acid. The morphological and particle size study evaluated by SEM technique according that the nano-silica and nano-SSA formed at nanoscale (below 200 nm). Nano-SSA have receiving a great interest from researchers and becomes the best solid support for the organic transformations due to their adequate catalytic

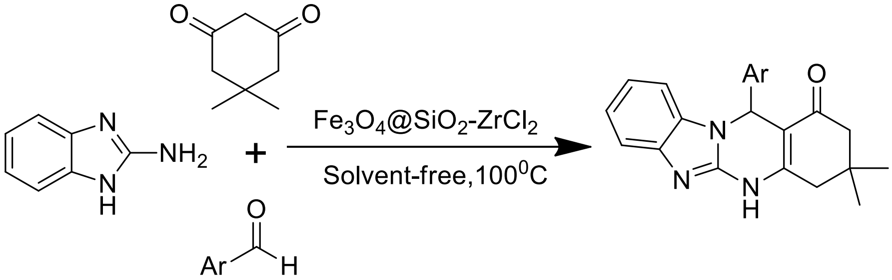

Scheme 30 Synthesis of Tetra-hydrobenzimidazo[2,1-b]quinazolin-1(2*H*)-one derivatives

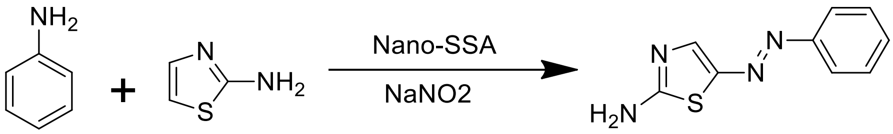

Scheme 31 Synthesis of azothiadiazoles

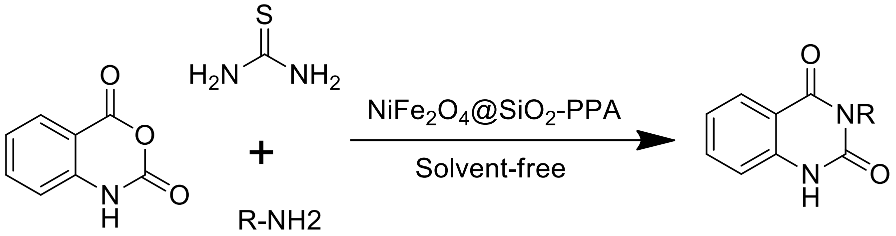

Scheme 32 Synthesis of 2-thioxoquinazolinones derivatives

performance; stability under harsh reaction conditions, large surface to volume ratio, renders a plurality of active sites, inertness under the reaction progression and tunable pore structure. The authors observed excellent results by using different composition of catalyst from 0.01 to 0.05 gm increases the conversion of product formation. The chosen synthesis method is effective, green, inexpensive, and satisfactory to give the products in high yield with an excellent purity in short times under mortar-pestle grinding. At the end the catalyst was recovered by filtration and washing treatment with distilled water. Thus, the authors observed the nano-SSA catalyst is having enough stability and can be reused up to four consecutive runs [92].

H. Eshghi et al. demonstrated the simple new catalytic method, polyphosphoric acid functionalized silica-coated magnetic nanoparticles with core–shell structure ($NiFe_2O_3@SiO_2$-PPA) as an acidic catalytic system for the one-pot 3C synthesis of 2-thioxoquinazolinones derivatives (Scheme 32) [93]. Authors reported new catalytic method, in which they used inorganic acid; polyphosphoric acid (PPA) for solid support but PPA is homogeneous, due to this it is going difficult to separate from reaction mixture to overcome this drawback, they did to support this acid on silica-coated MNPs. According to VSM analysis, $NiFe_2O_4$ NPs have magnetic saturation value is 16.71 emu g^{-1} at r.t; these particles shows high permeability in magnetization, leads easy magnetic separation. At the end, Authors claimed that the catalyst recovered and reused five courses without reduction in its catalytic performance.

Ionic-liquid supported NPs

Ionic-liquid is an innovative greener fluids have gained a fully concentration from scientific community. ILs shows best performance than conventional volatile solvents and exhibiting unique properties. Magnetic Fe_2O_3 NPs supported with IL-Ag complex (Ag^+ containing 1-trimethoxysilylpropyl imidazolium chloride

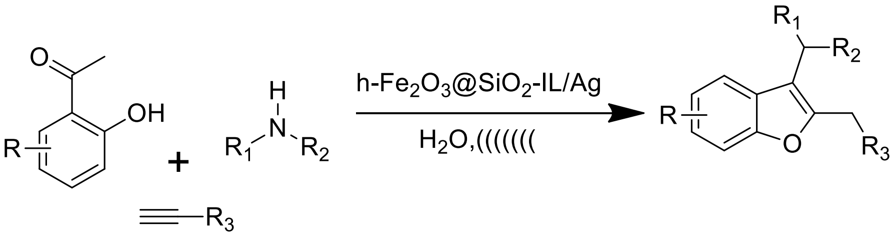

Scheme 33 Synthesis of benzo[*b*]furan

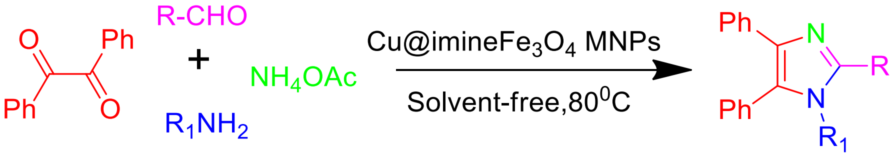

Scheme 34 Synthesis of 1,2,4,5-tetrasubstituted imidazole derivatives

ionic-liquid catalyst and denoted their use as heterogeneous catalyst for upgrading ultrasonic-assisted synthesis of benzo[*b*]furans(Scheme33).

Sadjadi; group. Thwin et al. reported, Cu@imine/Fe3O4 MNCs was used for the synthesis of biological active poly-substituted 1,2,4,5-tetrasubstituted imidazole derivatives (Scheme 34). Nanocatalysts was magnetically separated and reused for a minimum of six turns [95].

Furthermore, catalyst diffused in the reaction media, simply magnetically eliminated from reaction mixture, and recycled many times lacking substantial gain of its activity.

Metal–organic framework (MOF) supported NPs

In last decades, metal–organic frameworks (MOFs) fusion of metal ions and polyfunctional organic ligands are a novel trend of porous crystalline materials that attribute great potential in different sectors because of their high porosity, large surface area and adjustable pore size. Zhang HY et al. prepared MOF supported ($NiFe_2O_4$@MOF) catalyst. This magnetically separable catalyst adequate superior catalytic activity for the synthesis of 2-substituted alkyl and aryl (indolyl) kojic acid

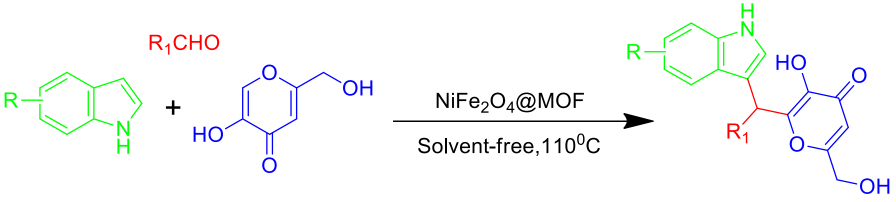

Scheme 35 Synthesis of 2-substituted alkyl and aryl (indolyl) kojic acid derivatives

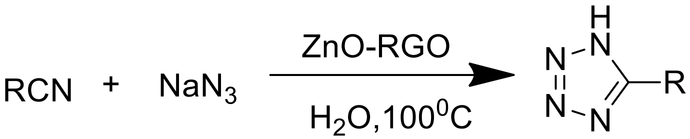

Scheme 36 Synthesis of 5-substituted-1H-tetrazoles

derivatives (Scheme 35) under solvent-free technique. Authors claimed that, the catalyst was magnetically separated and reutilized for several runs, without lack in its catalytic activity [96].

MOF supported Ni–Pt bimetallic nanoparticles as a vastly effectual catalyst for hydrogen generation from hydrous hydrazine in the presence of NaOH. In this said protocol highly diffused Ni–Pt bimetallic NPs with adjustable size with an standard dimension of 2 nm have been strongly paralyzed by the frameworks of ZIF-8, which shows huge catalytic activity. Authors have made various molar ratios (50:50, 60:40, 70:30, 80:20, 90:10) from nickel chloride and potassium tetra-chloroplatinate, respectively, between which (80:20) present the best turnover frequency (TOF). The Morphological study of synthesized MOF supported Ni–Pt NPs was evaluated by XRD, TEM, XPS, and BET analysis for specific surface area [97]. There are consistent necessity for research on polyfunctional nanocatalyst for green and sustainable protocol for organic transformations, for development of more efficient and green chemical processes for economic and ecological point of view.

Graphene oxide-framework (GOF) supported NPs

Graphene oxide (GO) acts as a best support for encapsulation of MNCs due to its 2D plate-like structure and large specific surface area. GO acquire rich oxygen containing functionalities such as carboxyl, epoxide, hydroxyl, which makes GO as an absorbing assistance to supply co-valent attachment of different specific groups. Clarina and Rama reported [3+2] cycloaddition of nitriles with sodium azide (Scheme 36) using ZnO NPs anchored on reduced graphene oxide (ZnO-RGO) and green solvent (water). The catalyst was removed by easy filtration from reaction [98].

Sinha and team have described the synthesis of 2,4,5-trisubstituted imidazole by using graphene oxide supported gold nanocatalyst in aqueous media. Catalyst can be easily regained for the successive reactions and reused without lacking of activity. Zhang and group derived magnetically separable GO supported molybdenum (Fe_3O_4/GO–Mo) catalyst for synthesis of spiro-oxindole dihydropyridines (Scheme 37) in the presence of eutectic solvents based on choline chloride and urea. At the end, the catalyst was magnetically separated and reutilized for eight times without remarkable unchanged results in its catalytic performance [99].

Graphene quantum dots (GQDs) supported NPs

GQDs; a latest luminescent nanomaterial having zero-dimension (0D), member of carbon and grapheme family, consist of single to few layers of graphene-sheets

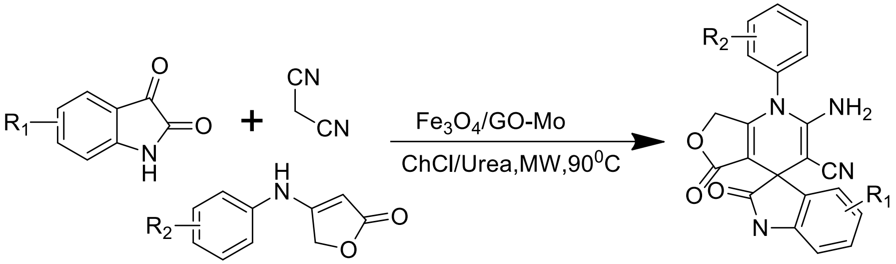

Scheme 37 Synthesis of spiro-oxindole dihydropyridines

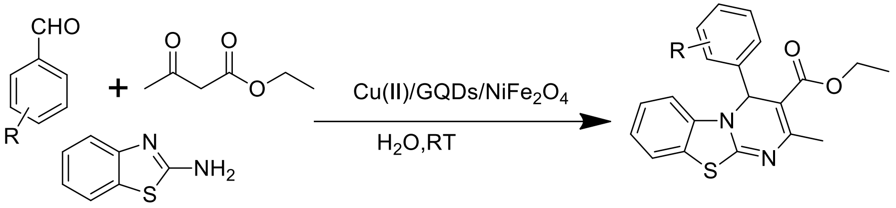

Scheme 38 Synthesis of 4*H*-pyrimido[2,1-b]benzothiazoles using Cu(II)/GQDs/$NiFe_2O_4$ NPs

with lateral dimensions of < 10 nm. GQDs based materials are gaining more attention due to its peculiar chemical/physical properties; such as low-toxicity, chemical inertness, solubility, functionality, crystallinity, two-dimensionality, biocompatibility [106]. Now a days, preparation of highly efficient nanocatalyst for organic transformations become a major challenging task. It is proven by the modification of the nanocatalyst supported with zero-dimension nanographenes GQDs have special characteristics that it avoid aggregation of fine particles and enhance the active surface area also improves catalytic properties. K. Khazenipour et al. designed a novel magnetically remediable catalytic system (Cu(II)/GQDs/$NiFe_2O_4$) modified by graphene quantum dots and stabilized by Cu(II). The immobilization of nano-$NiFe_2O_4$ on GQDs leads to a multipurpose nanoscaffold (Cu(II)/GQDs/$NiFe_2O_4$) with efficient catalytic activities for green production of 4H-pyrimido [2,1-b] benzothiazoles derivatives (Scheme 38)[107]. Prepared magnetic heterogeneous nanocomposite was analyzed by UV–Vis, FT-IR, XRD, EDS, VSM,TEM, and ICP, etc. TEM analysis reveals that the mean size of Cu(II)/GQDs/$NiFe_2O_4$ NPs are approximately below than 40 nm. Magnetic characteristics are proven by VSM studies; Cu(II)/GQDs/$NiFe_2O_4$ NPs have (60.82 emu g^{-1}) magnetization values, which indicates that the nanocatalyst has high magnetic properties. Therefore, easily isolated by a magnet. At the end, Authors claim that catalyst recovered five times without any reduction in its activities. Finally, authors proves that the environment of grapheme quantum dots supported $NiFe_2O_4$ nanomagnetic particles stabilized by copper(II)/GQDs/$NiFe_2O_4$ NPs consistent with the green chemistry principles.

Furthermore, R. Deilam et al. reported synthesis of 1,2,3-triazoles (Scheme 39) by using Cu(II)-supported grapheme quantum dots modified $NiFe_2O_4$ nanocatalyst

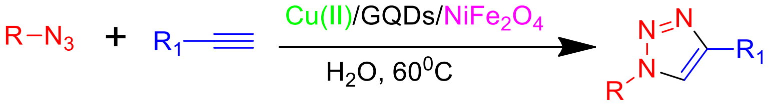

Scheme 39 Synthesis of 1,2,3-triazoles using Cu(II)/GQDs/$NiFe_2O_4$ NPs

as a innovative catalytic system (Cu(II)/GQDs/$NiFe_2O_4$). Heterogeneous solid GQDs supported porous environment reduce particle aggregation also generates a specific adsorption site which impact in rapid catalytic efficiency. The catalytic execution was explored in synthesis of bioactive 1,4-disubstituted 1,2,3-triazoles derivatives [108] rapidly in aqueous medium with 98% yield. At the end Authors said that, the catalyst was separated by outer magnet and recovered by five runs without failure in its performance.

As well, S. Monajjemifar et al. discussed the preparation of Cu(II) supported grapheme quantum dots modified $NiFe_2O_4$ as novel magnetically retrievable catalytic system Cu(II)/GQDs/$NiFe_2O_4$ as a proficient nanocatalyst. When the particle size reduced to nanoscale, aggregation of particles into small cluster; results in reduction in catalytic activity and to overcome this problem and simultaneously acquire nanoscale size it is need to restrict the particle growth reaction. The porous environment of GQDs support not only reduce particle aggregation but also achieve specific area which generates a specific adsorption site alternate faster catalytic activity and lead to multifunctional nanoscaffold.

Synthesized nanocatalyst was properly validating using discrete methods through UV–Vis, FT-IR, XRD, EDS, ICP, TGA, etc.[109]. The prepared graphene quantum dots have light-conducting characteristics which proven by UV–Vis and fluorescence spectroscopy. In fluorescence spectra of GQDs; in which the GQDs were excited at wavelengths of 360, 380, 400 nm and the exact fluorescence emission peaks were observed at 454, 463, 469 nm, respectively. These emission peaks indicates the red shift with a promoting in the excitation wavelengths (360–400 nm), and the color of GQDs aqueous solution is weak yellow under visible light but when excited by UV-light at 365 nm it appeared blue. The fluorescence spectra of GQDs/$NiFe_2O_4$ excited at 360, 380, 400 nm, and the exact fluorescence emission peaks were observed at 486, 483, 480 nm, respectively; due to this increasing excitation wavelength emission peaks indicates blue shift. This differentiation in fluorescence intensity of GQDs and GQDs/$NiFe_2O_4$ NPs determine the change in surface characteristics. The FT-IR spectroscopy was employed to prove the exterior framework and functional groups of nanocatalyst. In which, the broad peak at 3362.97 cm^{-1} indicates the presence of hydroxy (O–H) bond. The bonds placed at 2981 cm^{-1} and 1450 cm^{-1} are related to C–H bond. The peak located at 1001.35 cm^{-1} and 1415.34 cm^{-1}, 1594.81 cm^{-1} would be result of vibrational stretching of the C–O–C bond and skeletal vibrations of aromatic rings in GQDs, respectively. The adsorption bands positioned at 550.64 cm^{-1} and 685.24 cm^{-1} are co-related to Ni–O and Fe–O bonds, proves that the successful synthesis of magnetic nanocatalyst ($NiFe_2O_4$). X-ray diffraction technique was accomplished to bring the data about crystallinity of the nanocatalyst. The chemical constitution of the prepared nanocatalyst was occupied by EDS analysis, which justifies the existence of

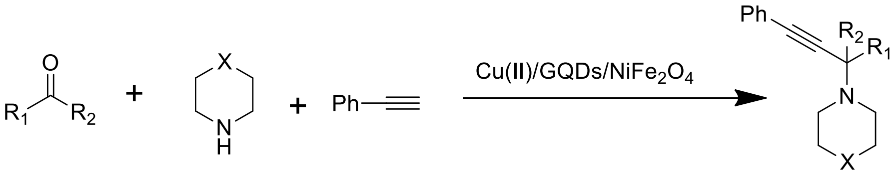

Scheme 40 Synthesis of propargylamines catalyzed by Cu(II)/GQDs/$NiFe_2O_4$ NPs

nickel, iron, oxygen, carbon, and copper elements in the catalyst structure. The ICP technique used to determined the quantity of Cu loading onto the nanocatalyst which was obtained 0.94 mmol g^{-1} GQDs surrounded by $NiFe_2O_4$ crystallites. The TGA analysis done on GQDs/$NiFe_2O_4$ NPs under N_2 atmosphere proffer confirmation of GQDs surrounded by $NiFe_2O_4$ NPs. Initial weight loss occurs at around 230–300 °C is about 30 wt %, which conclude that, the proportion of GQDs on GQDs/$NiFe_2O_4$ is about 30%. After proving the successful synthesis of nanocatalyst, Authors examined the catalytic capability of prepared nanocatalyst in the synthesis of propargylamines derivatives (Scheme 40). Propargylamines have three components linkage of amines, aldehydes, and alkynes called A^3 coupling; also considered as a useful key component in natural products and pharmaceutical constituents. Authors were strictly followed the green chemistry principles; solvent-free technique, low catalyst percentage, less reaction time, easy workup, easy recovery (5 runs) and reusability without failure in its efficiency, atom economy (95%) with high (TON:33.93) and (TOF:1.13 min^{-1}) values.

Graphitic carbon nitride (GCN), boron nitride (BN), MXenes supported NPs

Research into graphitic carbon nitride is still relatively new, and ongoing studies continue to explore its properties and potential applications in various fields. GCN, often abbreviated as g-C_3N_4 or g-CN is a two-dimensional polymeric material having layered graphite-like structure composed of carbon, nitrogen, and hydrogen atom. The catalytic performance of conventional heterogeneous catalysts is weak due to its low surface area; one of the promising solution for that by employing appropriate stabilizing support material to avoid metal nanoparticles aggregation which increases the surface area of catalyst by reducing their particle size; ultimately enhance the catalytic performance. Therefore, GCN; a sustainable stable, and cost-effective solid supports with tuned properties like basic surface functionalities, H-bonding, semiconductor, photoelectronics, etc., and used for catalysis, energy storage, and many other applications [110]. Lately, the H. G. Sampatkumar et al. synthesized biofabricated palladium nanoparticles grafted on banana leaves extract modified graphitic carbon nitride [Pd NPs@g-C_3N_4-BLE] as a very efficient and reusable nanocatalysts for reduction in various nitroarenes (Scheme 41). In this project, banana leaf extract and hydroxyl substituted graphitic carbon nitride (g-C_3N_4–OH) as a stabilizing and supporting materials; due to this eco-friendly support, this protocol become more effective inside the environmental aspects. The synthesized nanoparticles was characterized by diverse methods as FT-IR, XRD, GC-MS, ICP-OES, TG/DTA, UV–Vis, FE-SEM, EDX, HR-TEM, and BET analysis.

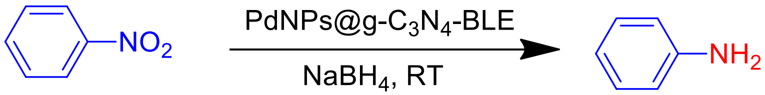

Scheme 41 Reduction in nitrobenzene by using PdNPs@g-C_3N_4-BLE NPs

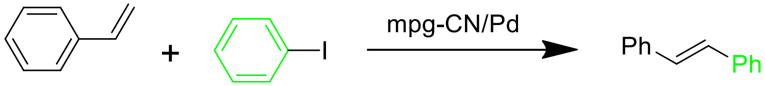

Scheme 42 Mizoroki–Heck coupling reaction by using mpg-CN/Pd NPs

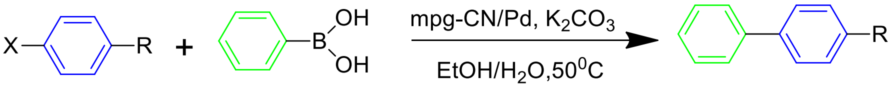

Scheme 43 Suzuki–Miyaura coupling reaction by using mpg-CN/Pd NPs

The heterogeneity study of PdNPs@g-C_3N_4-BLE nanocatalyst was carried out by hot filtration test [111].

Also, E. Kalay well-studied the catalytic performance of palladium nanoparticles supported on mesoporous graphitic carbon nitride (mpg-CN/Pd NPs) for the C–C bond formation Heck and Suzuki cross-coupling reactions (Scheme 42,43). Synthesized heterogeneous nanocatalyst was examined by different characterization techniques. The highly dispersed Pd NPs with an average particle size less than 50 nm, was observed in TEM images [112].

Boron nitride (BN) is a chemical compound composed of boron and nitrogen atom. The most common forms of BN are first is Hexagonal boron nitride (h-BN), has a layered structure similar to graphite each layer consist of covalently bonded hexagonal rings of alternating boron and nitrogen atoms. h-BN is more thermally and chemically stable. Second is Cubic boron nitride (c-BN) has a zinc-blend crystal structure similar to diamond, with boron and nitrogen atoms forming a 3D network. It is often referred as boron nitride diamond due to its hardness and strength. Both h-BN and c-BN possesses remarkable properties that make them useful in diverse fields [113]. Since we already know, small-sized catalysts are prostrate to agglomeration in catalytic reactions, leads to catalyst deactivation. BN can effectively overcome this trouble as they retain the thermal stability of h-BN with increased specific surface area. Due to this BN can provide a more stable loading space for metal nanoparticles as compared to other inorganic materials. BN supported NPs acts as proficient catalysts in organic reactions which promotes chemical transformations without being consumed in the process.

MXenes are a family of two-dimensional materials consisting of transition metal carbides, nitrides, or carbonitrides. They are synthesized by selectively elimination of the ‘*A*’ element from MAX phases, which are layered ternary compounds. The resulting MXene layers have excellent electrical conductivity, high surface area, and tunable surface chemistry [114]. Both boron nitride and MXenes offer exciting

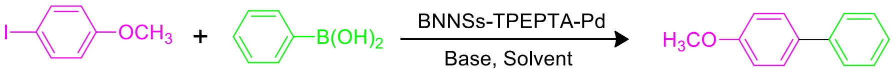

Scheme 44 Suzuki–Miyaura cross-coupling reaction by using BNNSs-TPEPTA-Pd NPs

opportunities for advancing organic synthesis and addressing challenges related to catalysis, green chemistry, and materials developments. Recently, T. Zhang et al. investigated the anchoring palladium nanoparticles on tris(pentaethylene-pentamine) triazine modified boron nitride nanosheets BNNSs-TPEPTA-Pd NPs; 2D heterogeneous catalyst for Suzuki–Miyaura cross-coupling reaction (Scheme 44). Synthesized BNNSs-TPEPTA-Pd NPs was analyzed by XRD, SEM, TEM, TGA, and XPS. Mostly, XPS was used to determine the elemental composition. Authors revealed that, the distribution of Pd NPs (average size 50 nm) was relatively dispersed and uniform more palladium atoms exposed on the surface of nanoparticles leads increasing the efficiency of Palladium; Authors had proven the BNNSs-TPEPTA-Pd NPs were relatively high catalytic activity for Suzuki-coupling reaction. Moreover, BNNSs-TPEPTA-Pd NPs was recovered by simple filtration and recycled up to eight run. The XRD pattern and TEM images are unchanged after the eight run revealed the good catalytic efficiency of the catalyst [115].

Dendrimer-supported NPs

Dendrimers are large nanoscale polymeric molecules and highly ordered tree-like branched structure. Dendrimers have three major portions, a core, an inner shell, and an outer shell, often adopt a spherical three-dimensional morphology. They form very uniform and monodispersed spheroid or globular macromolecular nanostructure with size from 1 to 10 nm. Dendrimer, is non-immunogenic, non-toxic, and biodegradable formerly used in cancer therapy, drug delivery, and catalysis [116]. The synthesis of dendrimer-supported nanoparticles for catalysis has some noticeable influence as; producing well-defined nanoparticles with uniform shape and structure, restricting agglomeration causing in surface area, enhancing catalytic properties of the catalyst, comfortable recover capacity, reutilization along with their eco-friendly nature due to these beneficially factors; recently, the heterogeneous dendrimer-supported nanocatalyst gained much attention and have been effectively used in several organic reactions. There are many dendritic molecules like poly (propylene imine), poly (L-lysine) (PLL), triazine, etc. Among those triazine-based dendrimers have received much attention due to cost-effective and selective reactivity of the cyanuric chloride as the relevant parent material. Currently, F. Moeinpour et al. investigated the study of Cu(II)/hydroxyl terminated triazine-based dendrimer Cu(II)/TD as a efficacious recoverable heterogeneous catalytic system for the construction of cyclic carbonate derivatives (Scheme 45) via CO_2 chemical fixation reaction. The Cu(II)/TD nanocatalyst was recognized by diverse methods, TEM, FT-IR, TGA, SEM, EDS, XRD, ICP techniques. The thermal stability of synthesized (Cu(II)/TD) catalyst was determined by TGA analysis, the major weight loss observed is 18% up to 150–200 °C, is related to elimination of water. Interestingly, when the morphology of the Cu(II)/TD catalyst was studied by SEM and TEM, authors

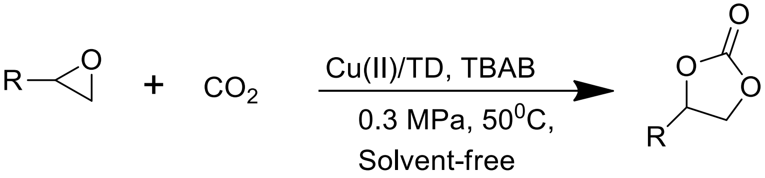

Scheme 45 Synthetic route for the cyclic carbonates using Cu(II)/TD catalyst

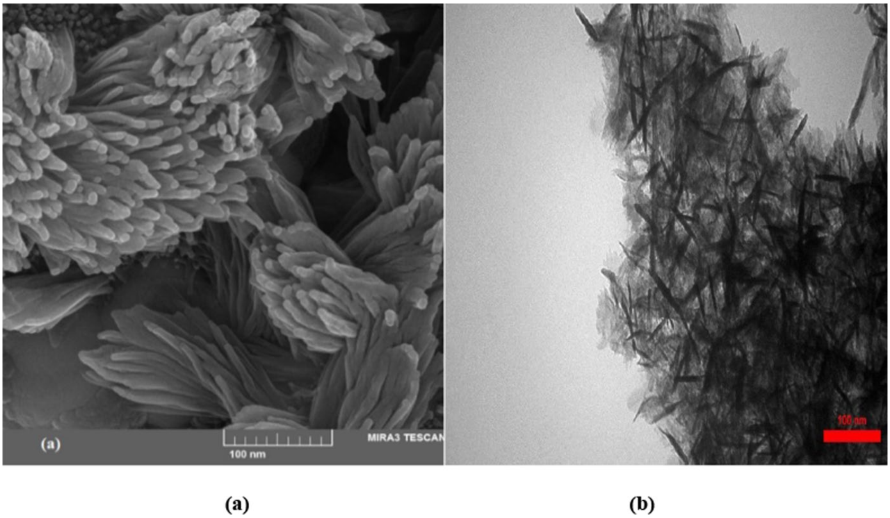

(a) (b)

Fig. 4 SEM image of Cu(II)/TD NPs (**a**), TEM image of Cu(II)/TD NPs (**b**). Copyright 2022, Springer Nature. Reprinted from ref. 119 with permission

observed the strip and filament structure of the dendrimer (Fig. 4a and b). According to TEMimages the dendritic and branching structure of the Cu(II)/TD catalyst is well visible, with middle size is less than 100 nm. The amount of Cu in Cu(II)/TD measured by ICP analysis is 0.90 mmol/g. UV–Vis spectra of catalyst, the band at 286 nm indicated the presence of Cu(II) species. After validating the successful loading of Cu(II) with, TD; authors were examined its catalytic ability for the reaction of diverse epoxides and CO_2 catalyzed by Cu(II)/TD (0.045 mol%) at 50 °C, 0.3 MPa of CO_2 pressure and 10 mol% of TBAB with solvent-less conditions [117]. At the end, Authors claimed that, after the reaction was terminated, the simple filtration process was used for isolation of catalyst and then reapplied for five times without any alteration in its proficiency. High stability, recoverability, and efficiency of the Cu(II)/TD; as a catalytic agent make this project reliable in the context of cyclic carbonates preparation.

Also, S. Ghoreishi et al. discussed the preparation of Cu(II)/TD nanocatalyst for the solvent-free synthesis of primary amides through MW-assisted Beckman rearrangment (Scheme 46). The ending, Authors proved the recycle capability of catalyst by taken the FT-IR spectrum and SEM image of reprocessed Cu(II)/TD NPs (5th run), demonstrated that its particles sustain their size and morphology without any considerable

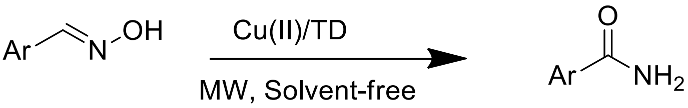

Scheme 46 Beckman rearrangement by Cu(II)/TD NPs

change in chemical structure [118]. Lately, S. Javdan et al. group further expanded the study of same Cu(II)/TD as an proficient recoverable nanocatalyst for the synthesis of tetrazole derivatives (Scheme 47) in outstanding yields (95%) [119].

As well, S. Khodsetan et al. discussed, the preparation, characterization and reapplication of Cu(II)-TrDen@nSiO$_2$ as a retrievable catalytic system for green formation of propargylamines (A^3 coupling of phenyl acetylene, benzaldehyde and morpholine) (Scheme 48). The morphological structure of nanocatalyst was studied by SEM analysis, that Cu(II)-TrDen@nSiO$_2$ NPs are globular. TEM analysis revealed that, the electron density of Cu(II) is greater than the nano-silica due to this, darker region seen in Cu(II)-TrDen@nSiO$_2$ images; that revealed to Cu(II) and uncolored parts were silica. Also, the TEM analysis confirmed the mean size of nanocatalyst approximately below than 40 nm. The quantity 0.67 mmol/g of Cu loading onto the nanocatalyst was measured by ICP technique. Authors claimed that, the nanocatalyst was isolated by filtration and reapplied in subsequent reactions. To explore the leaking of copper and recyclability capacity the ICP analysis of the catalyst taken after the fifth cycle of the reaction which did not show significant reduction in the Cu quantity [120].

Overall, the use of supported nanoparticles in organic synthesis offers numerous advantages, including improved reaction efficiency, selectivity, and recyclability, making them valuable tools for designing sustainable and efficient synthetic routes in various chemical process (Tables 4 and 5).

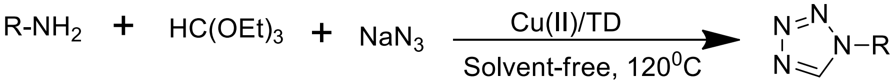

Scheme 47 Synthesis of tetrazoles using Cu(II)/TD NPs

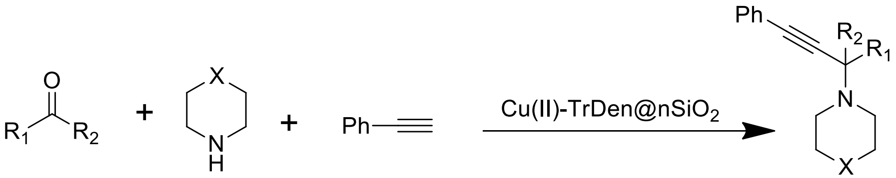

Scheme 48 Synthesis of propargylamine by using Cu(II)-TrDen@nSiO$_2$ NPs

Table 4 Supported NPs for organic transformations

Sr No	Supported NPs	Condition	Features	Yield %	NPs Size (nm)	TOF h^{-1}	References
1	Fe_3O_4@SiO_2-$ZrCl_2$	100 °C Solvent-free	Synthesis of tetrahdro- benzimidazo quiniline	80	–	–	[91]
2	Nano-SSA (0.05 gm)	$NaNO_2$, RT Solvent-free, 5 min	Synthesis of azothiadia- zoles derivatives	71–91	< 200	–	[92]
3	h-Fe_2O_3@SiO_2-IL	H_2O	Synthesis of benzofuran	85	–	–	[94]
4	Cu@imine Fe_3O_4 (0.36 mol %)	Solvent-free, 80 °C 35 min	Synthesis of 1,2,4,5-tetra substituted imidazole	95	–	–	[95]
5	$NiFe_2O_4$@MOF	Solvent-free 110 °C	Synthesis of 2-substituted alkyl aryl(indolyl) kojic acid	–	–	–	[96]
6	ZnO-RGO (20 W %)	H_2O, 100 °C 2 h	Synthesis of 5-substituted-(1H)-tetrazoles	94–96	–	–	[98]
7	Fe_3O_4/GO-Mo	ChCl/Urea MW, 90 °C	Synthesis of spiro-oxindole dihydropyridines	–	–	–	[99]
8	Au@ZrO_2	H_2O, hv 40–80 °C	Hydrogenation of un- saturated aromatics	70–100	7	–	[100]
9	Pd-rGOF	H_2O, 100 °C	Tsujit-Trost reaction	> 99	3–4	–	[101]
10	Fe_3O_4@Zeolite-SO_3H	Solvent-free	Synthesis of pyrimidine derivatives	9857	–	–	[102]
11	AgOTf (10 mol%)	$(CH_2)_2Cl_2$,80 °C 4 h	Synthesis of Furo[2,3-b]pyran-2-one	88–93	–	–	[103]
12	Ni/RGO	DMF, K_2CO_3, 100 °C	C-S Cross-coupling reaction	97	–	–	[104]
13	Pd/PEG	–	Reduction in nitrobenzene	98	–	–	[105]
14	Cu(II)GQDs/$NiFe_2O_4$	H_2O, rt	Synthesis of benzothiazoles	98	40	–	[107]
15	Cu(II)GQDs/$NiFe_2O_4$	H_2O, 60 °C	Synthesis of triazoles	95	40	–	[108]
16	Cu(II)GQDs/$NiFe_2O_4$	Solvent-free, 100 °C	Synthesis of propargylamines	98	40	–	[109]
17	PdNPs@g-C_3N_4-BLE	$NaBH_4$, rt EtOH:H_2O(1:1)	Reduction in nitroarnes	88	< 50	–	[111]
18	mpg-CN/Pd	K_2CO_3, EtOH/H_2O,50 °C	Suzuki–Miyaura coupling reaction	95	< 50	–	[112]
19	BNNSs-TPEPTA-Pd	Base, solvent	Suzuki–Miyaura coupling reaction	98	50	–	[115]
20	Cu(II)/TD	TBAB, 50 °C, Solvent-free	Cyclic carbonates	96	< 100	–	[117]
21	Cu(II)/TD	MW, solvent-free	Beckman rearrangement	98	< 100	–	[118]
22	Cu(II)/TD	Solvent-free, 120 °C	Synthesis of tetrazoles	95	< 100	–	[119]
23	Cu(II)-TrDen@$nSiO_2$	Solvent-free, 100 °C	Synthesis of propargylamine		40	–	[120]

Table 5 Related chart for metal, metal oxide, bimetallic and supported NPs for organic transformations

Characteristics	Metal NPs	Metal oxide NPs	Bimetallic NPs	Supported NPs
1.Catalyst used	Cu[12], Pd[15], Au[16], Pt[17] (noble) metals are used	All types of metals, (transitions, innertransitions, etc.) is used [24]	Combination of any two metals (transitions, inner- Transitions, etc.) is used [63]	All type of metal (transition, inner- transition, etc.) Is used [83]
2. Catalyst in reaction medium	i) Homogeneous [16] [14] ii) Heterogeneous	i) Homogeneous or ii) Heterogeneous [33]	i) Heterogeneous [71]	i) Heterogeneous [108]
3. Aggregarion of catalyst	Observed [15]	Observed [40]	Less [73]	Very less [111] [117]
4. Catalyst separation method	i) Centrifuge	i) Centrifuge ii) magnetically [49]	i) Centrifuge ii) magnetically [71]	i) Centrifuge ii) magnetically [94] [107] iii) Simple filtration [115] [120]
5. Leaching of catalyst (after completion of rea.)	Less	Less	Less	Very Less [120]
6. Recyclability	Recyclable	Recyclable	Recyclable	Recyclable
7. Efficiency	High	High	High	Very High

Conclusion

In this review we revealed detail motif about nanoparticles, synthesis, classification, and catalytic applications. In this perspectives, we try to present current advancement in the synthesis of various types of nanoparticles such as Metal NPs, Metal oxide NPs, Bimetallic NPs, and Supported NPs; can be synthesized from various methods and their broad applicability for green and sustainable organic transformations. There are some limitations and challenges in this area that need to be addressed for their implementation. Some of these includes, synthesis complexity and stability, reactivity control, cost, toxicity and environmental impact, catalyst separation and recovery, scaling-up, health and safety concern, etc. Addressing these limitations and challenges, ongoing research is focused on successful development and application of nanocatalyst. Progressively existence of nanocatalysts has appeared as a fragment of green chemistry, which generates a lot of positive outcomes and used for swift development in the field of organic transformations, sensing technology, energy storage, catalysis, and medicinal applications. In a current scenario, Covid-19 pandemic which will go into history, and how world has fought against it; which also can be partially resolved through nanotechnology. There is need to conducted more promising studies on synthesis and applications of NPs as a catalyst for large-scale industrialized progressions to improve innovative, active and selective ideal catalyst in the upcoming future. This review, will make a great collection in the area of organic synthetic nanotechnology via green media and sustainable environmental path will be the foundation for a colorful future of research as like rainbow and ultimately become the healthy environmental future of research in this fields.

Acknowledgments R. P. Patil is thankful to the Chhatrapati Shahu Maharaj Research, Training and Human Development Institute (SARTHI), Government of Maharashtra; India, for the Chhatrapati Shahu Maharaj National Research Fellowship (CSMNRF-2021) for their great support. Also, especially thanks to Dr. K. N. Alasundkar, and Dr. V. A. Kalantre for their helpful suggestions.

Author contributions RPP contributed to conceptualization, and execution of data, analysis of result, and writing of the manuscript. KNA contributed to assessing, invigilation, formulate hypotheses, design and Implementation of data, editing of the manuscript, and in-charge of overall research design and planning. VAK contributed to guidance, and supervision.

Funding Chhatrapati Shahu Maharaj Research, Training and Human Development Institute (SARTHI), Government of Maharashtra; India, for the Chhatrapati Shahu Maharaj National Research Fellowship (CSMNRF-2021).

Data availability Not Applicable.

Declarations

Conflict of interest There are no conflicts of interest to declare.

Ethical approval Not Applicable.

References

1. R.S. Varma, A.H. Moores, Green chem. **16**, 2027 (2014)
2. M.B. Gawande, P.S. Branco, R.S. Varma, Chem. Soc. Rev. **42**(8), 3371 (2013)
3. V. Polshettiwar, R.S. Varma, Green chem. **12**(5), 743 (2010)
4. R.S. Varma, ACS Sustainable Chem. Eng. **11**(4), 5866 (2016)
5. B.M. Sharma, R.S. Atapalkar, A.A. Kulkarni, Green Chem. **21**(20), 5639 (2019)
6. H. Hamrayev, K. Shameli, M. Yusefi, S. Korpayev, J. Res. Nanosci. Nanotechnol. **3**(1), 1 (2021)
7. S.R. Attar, S.B. Kamble, Nanoscale **14**, 16761 (2022)
8. D. Astruc, Inorg. Chem. **46**(6), 1884 (2007)
9. T. Kitanosono, K. Masuda, P. Xu, S. Kobayashi, Chem. Rev. **118**(2), 679 (2018)
10. S. Praharaj, S. Nath, S.K. Ghosh, S. Kundu, T. Pal, Langmuir **20**(23), 9889 (2004)
11. T. Itoh, T. Mase, Org. Lett. **9**(18), 3687 (2007)
12. A. Zamani, A.P. Marjani, A. Nikoo et al., Inorg. Nanomet. Chem. **48**, 176 (2018)
13. P. Devendar, R.-Y. Qu, W.-M. Kang, B. He, G.-F. Yang, J. Agric. Food Chem. **66**(34), 8914 (2018)
14 L. Qiu, Y. Jin, Y. Gong et al., Chem Sci. **9**, 676 (2018)
15. S. Sawoo, D. Srimani, P. Dutta et al., Tetrahedron **65**, 4367 (2009)
16. W. Guo, R. Pleixats, A. Shafir, Chem. Asian J. **10**(11), 2437 (2015)
17 R. Saha, G. Sekar, Appl. Catal. B **250**, 325 (2019)
18. M.B. Deshmukh, K.N. Alasundkar, D.K. Salunkhe, S.A. Sankpal, J. Chem. Pharm. Res. **2**(4), 437 (2010)
19. S. Ahammed, A. Saha, B.C. Ranu, J. Org. Chem. **76**(17), 7235 (2011)
20. F. Alonso, Y. Moglie, G. Radivoy, Acc. Chem. Res. **48**(9), 2516 (2015)
21. M.S. Islam, M.A.S. Mia, SN Appl. Sci. **2**, 1 (2020)
22 W. Feng, T. Huang, L. Gao et al., RSC Adv. **8**, 6288 (2018)
23. G.A. Price, A.K. Brisdon, K.R. Flower, R.G. Pritchard, P. Quayle, Tetrahedron Lett. **55**, 151–154 (2014)
24. M. Saha, A.K. Pal, S. Nandi, RSC Adv. **2**(16), 6397–6400 (2012)
25. W. Tian, H. Lu, L. Li, Nano Res. **8**(2), 382 (2015)
26. B. Liu, J. Liu, TrAC Trends Anal. Chem. **121**, 115690 (2019)
27. D.R. Miller, S.A. Akbar, P.A. Morris, Sens. Actuators B Chem. **204**, 250 (2014)
28. S.M. Dizaj, F. Lotfipour, M. Barzegar-Jalali, M.H. Zarrintan, K. Adibkia, Mater. Sci. Eng. C **44**, 278 (2014)
29. A.V. Nikam, B.L. Prasad, A.A. Kulkarni, Cryst Eng Comm. **20**(35), 5091 (2018)
30. S.R. Attar, B. Shinde, S.B. Kamble, Res. Chem. Intermed. **46**(10), 4723 (2020)
31. J. Xu, G. Li, L. Li, Mater. Res. Bull. **43**(4), 90 (2008)
32. T. Raj et al., ACS Sustain. Chem. Eng. **5**(2), 1468 (2017)
33. M.B. Deshmukh, K.N. Alasundkar, S.A. Sankpal, P.V. Anbhule, India J. Chem. **47**, 1915 (2008)
34. A. Hassanpour, R.H. Khanmiri, J. Abolhasani, Synth. Commun. **45**, 727 (2015)
35. B. Shinde et al., Chem. Select **3**(46), 13197 (2018)
36. B. Paul, S. Vadivel, S.S. Dhar, S. Debbarma, M. Kumaravel, J. Phy. Chem. Solid. **104**, 152 (2017)
37. M. Shojaie, J. Synth. Chem. **1**(2), 125 (2022)
38. Q. Xia et al., J. Org. Chem. **86**(14), 9914 (2021)
39. J. Safaei-Ghomi, H. Shahbazi-Alavi, Polycycl. Aromat. Comp. **40**, 1534 (2019)
40. J. Safaei-Ghomi, M.A. Ghasemzadeh, S. Zahedi, J. Mex. Chem. Soc. **57**, 1–7 (2013)
41. A. Awol, Saudi J. Biomed. Res. **2**, 10 (2017)
42. L.E. Oi, M.Y. Choo, H.V. Lee, H.C. Ong, S.B. Abd Hamid, J.C. Juan, Rsc Adv. **6**(110), 108741 (2016)
43. G. Brahmachari, S. Das, India. J. Chem. Sect. Org. Chem. Incl. Med. Chem. **52**, 387 (2013)
44. S. Kumar et al., Synth. Commun. **39**, 2271 (2009)
45. B. Palakshi Reddy, P. Iniyavan, S. Sarveswari, V. Vijayakumar, Chin. Chem. Lett. **25**(12), 1595 (2014)
46. M.-N. Chen, L.-P. Mo, Z.-S. Cui, Z.-H. Zhang, Current Opin. Green Sustain. Chem. **15**, 27 (2019)
47. B. Karami, S.J. Hoseini, K. Eskandari, A. Ghasemi, H. Nasrabadi, Catal. Sci. Technol. **2**(2), 331 (2012)
48. R. Hudson, Y. Feng, R.S. Varma, A. Moores, Green Chem. **16**(10), 4493 (2014)
49. O.V. Fedorova, Y.A. Titova, I.G. Ovchinnikova, Chem. Heterocycl. Compd. **57**(9), 900–904 (2021)

50. J. Safari, L. Javadian, Ultrason. Sonochem. **22**, 341 (2015)
51. R. Gurav, S.K. Surve, S. Babar, P. Choudhari, D. Patil, V. More, S. Sankpal, S. Hangirgekar, Org. Biomolecul. Chem. **18**(24), 4575 (2020)
52. S.A. Sankpal, M.B. Deshmukh, P.V. Anbhule, D.K. Salunkhe, K.N. Alasundkar, J. Chem. Pharm. Res. **2**(5), 574 (2010)
53. A. Awol, Saudi J. Biomed. Res. **2**(1), 10 (2017)
54. J. Safaei-Ghomi, M. Asgari-Keirabadi, B. Khojastehbakht-Koopaei, H. Shahbazi-Alavi, Res. Chem. Intermed. **42**, 827 (2016)
55. A. Saha, S. Payra, S. Banerjee, RSC Adv. **5**(123), 101664 (2015)
56. S.Z. Mohammadi, B. Lashkari, A. Khosravan, Surf. Interfaces **23**, 100970 (2021)
57. G. Patel, A.R. Patel, G. Maity, S. Das, S.P. Patel, S. Banerjee, Current Res. Green Sustain. Chem. **5**, 100258 (2022)
58. P.G. Kargar, G. Bagherzade, RSC. Adv. **11**, 23192 (2021)
59. V. Vairaperumal, M. Perumal, P. Sengodu, S. Shanumuganthan, M. Paramasivam, Chem. Select **4**(11), 3006 (2019)
60. A. Kumar, D. Saxena, M.K. Gupta, Green Chem. **15**(10), 2699 (2013)
61. S. Payra, A. Saha, S. Guchhait, S. Banerjee, RSC Adv. **6**(40), 33462 (2016)
62. R. Shrestha, K. Sharma, Y.R. Lee, Y.-J. Wee, Mol. Divers. **20**(4), 847 (2016)
63. W. Yu, M.D. Porosoff, J.G. Chen, Chem. Rev. **112**(11), 5780 (2012)
64. R. Ghosh Chaudhuri, S. Paria, Chem. Rev. **112**(4), 2373 (2012)
65. R.N. Baig, R.S. Varma, Green Chem. **15**(2), 398 (2013)
66. B. Nakhjavan et al., Nanoscale **4**(15), 4571 (2012)
67. J.H. Park, Y.K. Chung, Dalton Trans. **18**, 2369 (2008)
68. K. Mishra, N. Basavegowda, Y.R. Lee, RSC Adv. **6**(33), 27974 (2016)
69. S. Li, J. Wang, J. Jin et al., Catal Lett **150**, 2409 (2020)
70. M. Saha, K. Pradhan, A.R. Das, RSC Adv. **6**, 55033 (2016)
71. J. Li, X.T. Li, E.Q. Ma, L.P. Mo, Z.H. Zhang, Chem Cat Chem. **6**, 2854 (2014)
72. L. Wang et al., J. Mater. Chem. C. **6**(8), 1996 (2018)
73. B. Shinde, S.B. Kamble, H.S. Jadhav, B.K. Karale, K.G. Kanade, A.S. Burungale, Chem. Select **3**(46), 13140 (2018)
74. S. Li, J. Wang, J. Jin et al., Catal. Lett. **150**, 2409 (2020)
75. C.M. Gabriel et al., Org. Process Res. Dev. **21**(2), 247 (2017)
76. R. Hudson, C.-J. Li, A. Moores, Green Chem. **14**(3), 622 (2012)
77. R. Ghahremanzadeh, Z. Rashid, A.H. Zarnani, H. Naeimi, Appl. Catal. A **467**, 270 (2013)
78. B. Shinde et al., Res. Chem. Intermed. **44**(5), 3097 (2018)
79. S. Handa, Y. Wang, F. Gallou, B.H. Lipshutz, Science **349**(6252), 1087 (2015)
80. S. Payra, A. Saha, S. Banerjee, RSC Adv. **6**(98), 95951 (2016)
81. B.A. Kumar, K.H.V. Reddy, B. Madhav, K. Ramesh, Y.V.D. Nageswar, Tetrahedron Lett. **53**(34), 4595 (2012)
82. H. Naeimi, Z. Rashid, A.H. Zarnani, R. Ghahremanzadeh, New J. Chem. **38**(1), 348 (2014)
83. M.J. Ndolomingo, N. Bingwa, R. Meijboom, J. Mater. Sci. **55**(15), 6195 (2020)
84. S.D. Karande, S.A. Jadhav, H.B. Garud, V.A. Kalantre, S.H. Burungale, P.S. Patil, Nanotechnol. Environ. Eng. **6**(2), 1 (2021)
85. B.K. Singh, S. Lee, K. Na, Rare Met. **39**(7), 751 (2020)
86. E.A. Monyoncho, S. Ntais, N. Brazeau, J.-J. Wu, C.-L. Sun, E.A. Baranova, Chem. Electro. Chem. **3**(2), 218 (2016)
87. J.L. Santos, C. Megías-Sayago, S. Ivanova, M.Á. Centeno, J.A. Odriozola, Chem. Eng. J. **420**, 127641 (2021)
88. M. d’Halluin et al., Carbon **93**, 974 (2015)
89. V. Shah et al., Sci. Total Environ. **573**, 661 (2016)
90. M.B. Deshmukh, K.N. Alasundkar et al., Der. Chemica. Sinica. **2**, 118 (2011)
91. F. Karnali, F. Shirini, New J. Chem. **41**, 11778 (2017)
92. V. Kamble, J. Jadhav, P. Piste, India J. Chem. **61**, 650 (2022)
93. H. Eshghi, M. Bakavoli, A. Khojastehnezhad, N. Zeinabi, S. Allameh, F. Moeinpour, Res. Chem. Intermed. **9**, 15966 (2019)
94. S. Sadjadi, M.M. Heravi, M. Malmir, Appl. Organomet. Chem. **32**, e4029 (2018)
95. M. Thwin, B. Mahmoudi, O.A. Ivaschuk, Q.A. Yousif, RSC Adv. **9**, 15966 (2019)
96. H.Y. Zhang, X.P. Hao, L.P. Mo, S.S. Liu, W.B. Zhang, Z.H. Zhang, New J. Chem. **41**, 7108 (2017)

97. A.K. Singh, Q. Xu, Chem. Cat. Chem. **5**(10), 3000 (2013)
98. T. Clarina, V. Rama, Synth. Commun. **48**, 175 (2018)
99. M. Zhang, Y.H. Liu, Z.R. Shang, Catal. Commun. **88**, 39 (2017)
100. Y. Huang et al., Catal. Sci. Technol. **8**(3), 726 (2018)
101. J. Liu et al., Nanoscale **8**(5), 2787 (2016)
102. M. Kalhor, Z. Zarnegar, F. Janghorban, S.A. Mirshokraei, Res. Chem. Intermed. **46**, 821 (2019)
103. S.S. Thorat, P. Kataria, R. Kontham, Org. Lett. **20**, 872 (2018)
104. D. Sengupta, K. Bhowmik, G. De, B. Basu, Beilstein J. Org. Chem. **13**, 1796 (2017)
105. G.K. Dasari, S. Sunkara, R.C.P. Gadupudi, Inorg. Nano. Met. Chem. **50**, 753 (2020)
106. P. Tian, L. Tang, K.S. Teng, S.P. Lau, Mater. Today Chem. **10**, 221 (2018)
107. K. Khazenipour, F. Moeinpour, F.S. Mohseni-Shahri, J. Chin. Chem. Soc. **68**, 1 (2020)
108. R. Deilam, F. Moeinpour, F.S. Mohseni-Shahri, Monatsh. Chem. Mon. **151**(7), 1153 (2020)
109. S. Monajjemifar, F. Moeinpour, F.S. Mohseni-Shahri, Catal. Lett. **151**, 1444 (2020)
110. J. Zhu, P. Xiao, H. Li, S.A.C. Carabineiro, A.C.S. Appl, Mater. Interfaces **6**, 19 (2014)
111. H. G. Sampatkumar, N. Rhakho, V. Kandathil, M. Kempasiddaiah, A. M. Shirahatti, R. B. Dateer, A. K. Samal, S. A. Patil, Catal. Lett. (2023)
112. E. Kalay, Synth. Commun. **52**(9–10), 1290 (2022)
113. D.V. Shtansky, A.T. Matveev, E.S. Permyakova, D.V. Leybo, A.S. Konopatsky, P.B. Sorokin, Nanomaterials **12**, 2810 (2022)
114. B. Anasori, Y. Gogotsi, Graphene 2D Mater. **7**(3–4), 75 (2022)
115. T. Zhang, G. Li, X. Zhang, L. Xu, Catal. Lett. (2022)
116. E. Abbasi, S.F. Aval, A. Akbarzadeh, M. Milani, H.T. Nasrabadi, S.W. Joo, Y. Hanifehpour, K. Nejati-Koshki, R. Pashaei-Asl, Nanoscale Res. Lett. **9**, 247 (2014)
117. F. Moeinpour, R. Khalifeh, M. Rajabzadeh, F. Rezaei, S. Javdan, Catal. Lett. **152**, 3679 (2022)
118. S. Ghoreishi, F. Moeinpour, Polycycl. Aromat. Compd. **43**(1), 740 (2023)
119. S. Javdan, F. Moeinpour, F.S. Mohseni-Shahri, Org. Prep. Proced. Int. **54**(4), 346 (2022)
120. S. Khodsetan, F. Moeinpour, Polycycl. Aromat. Comp. **42**(6), 3142 (2022)